การวิเคราะห์การล้าของอุปกรณ์ในสกรูสแตนเลสสำหรับกระดูกฟ่ามและสกรูสแตนเลสสำหรับกระดูกทึบที่ใช้ร่วมกับพอลิเมทิลเมทาคริเลต และในแผ่นดามกระดูกชนิดเอสโอพีที่ใช้ดามกระดูกสันหลังหักและเคลื่อนในร่างนิ่มสุนัข

นายมิ่งรัฐ เมฆวิชัย

วิทยานิพนธ์นี้เป็นส่วนหนึ่งของการศึกษาตามหลักสูตรปริญญาวิทยาศาสตรมหาบัณฑิต
สาขาวิชาศัลยศาสตร์ทางสัตวแพทย์ ภาควิชาศัลยศาสตร์
คณะสัตวแพทยศาสตร์ จุฬาลงกรณ์มหาวิทยาลัย
ปีการศึกษา 2560

Fatigue study of cancellous and cortical stainless steel screws used with polymethymethacrylate and the SOP plate system for the immobilisation of vertebral fracture and luxation in canine cadavers

Mr. Mingrath Mekavichai

A Thesis Submitted in Partial Fulfillment of the Requirements
for the Degree of Master of Science Program in Veterinary Surgery
Department of Veterinary Surgery
Faculty of Veterinary Science
Chulalongkorn University
Academic Year 2017

Thesis Title	Fatigue study of cancellous and cortical stainless steel screws used with polymethymethacrylate and the SOP plate system for the immobilisation of vertebral fracture and luxation in canine cadavers
By	Mr. Mingrath Mekavichai
Field of Study	Veterinary Surgery
Thesis Advisor	Assistant Professor Kumpanart Soontornvipart, D.V.M., Ph.D., D.T.B.V.S.

Accepted by the Faculty of Veterinary Science, Chulalongkorn University in Partial Fulfillment of the Requirements for the Master's Degree

.....Dean of the Faculty of Veterinary Science

(Professor Roongroje Thanawongnuwech, D.V.M., M.S., Ph.D., D.T.B.V.P.)

THESIS COMMITTEE

.....Chairman

(Assistant Professor Sumit Durongphongtorn, D.V.M., DVSc., D.T.B.V.S)

.....Thesis Advisor

(Assistant Professor Kumpanart Soontornvipart, D.V.M., Ph.D., D.T.B.V.S.)

.....Examiner

(Professor Marissak Kalpravidh, D.V.M., M.S., Ph.D., D.T.B.V.S.)

.....Examiner

(Associate Professor Chanin Kalpravidh, D.V.M., M.Sc., D.T.B.V.S.)

.....External Examiner

(Pichanun Linharattanaruksa, D.V.M., Ph.D)

มิ่งรัฐ เมฆวิชัย : การวิเคราะห์การล้าของอุปกรณ์ในสกรูสแตนเลสสำหรับกระดูกฟ่ามและสกรูสแตนเลสสำหรับกระดูกทึบที่ใช้ร่วมกับพอลิเมทิลเมทาคริเลต และในแผ่นดามกระดูกชนิดเอสโอพีที่ใช้ดามกระดูกสันหลังหักและเคลื่อนในร่างนิ่มสุนัข (Fatigue study of cancellous and cortical stainless steel screws used with polymethymethacrylate and the SOP plate system for the immobilisation of vertebral fracture and luxation in canine cadavers) อ.ที่ปรึกษาวิทยานิพนธ์หลัก: ผศ. น.สพ. ดร. กัมปนาท สุนทรวิภาต, 67 หน้า.

กระดูกสันหลังหักและเคลื่อนเป็นหนึ่งในสาเหตุหลักที่ทำให้เกิดความเสียหายของระบบประสาทในสุนัขและแมว วิธีการรักษาในปัจจุบันคือการใช้สกรูร่วมกับพอลิเมทิลเมทาคริเลตและการใช้แผ่นดามกระดูกชนิดเอสโอพี ภายหลังการยึดดามกระดูกสันหลังหักและเคลื่อนด้วยอุปกรณ์ยึดดาม แรงที่กระทำต่ออุปกรณ์ยึดดามจะเป็นแรงลักษณะกระทำเป็นรอบ แรงดังกล่าวต้องน้อยกว่าความทนแรงดึงของอุปกรณ์นั้นๆ อย่างมีนัยยะสำคัญและกระทำซ้ำมากพอ จะส่งผลทำให้เกิดการล้มเหลวจากการล้าตัวของอุปกรณ์ การศึกษานี้จึงทำการศึกษาเปรียบเทียบจำนวนรอบที่ทำให้เกิดการล้มเหลวของอุปกรณ์จากความล้าตัวและลักษณะการล้มเหลวของอุปกรณ์จากการล้าตัว โดยใช้เครื่องทดสอบความล้าที่ออกแบบขึ้นเองเพื่อวัตถุประสงค์เฉพาะ โดยทดสอบในอุปกรณ์ยึดดามสันหลัง 4 ชนิด ประกอบด้วย กลุ่มที่ 1 ใช้สกรูสำหรับกระดูกฟ่ามขนาด 3.5 มิลลิเมตรร่วมกับพอลิเมทิลเมทาคริเลตที่ใช้ในลักษณะการปั้นมือ (MP) กลุ่มที่ 2 ใช้สกรูสำหรับกระดูกฟ่ามขนาด 3.5 มิลลิเมตรร่วมกับพอลิเมทิลเมทาคริเลตที่ใช้เทคนิคกระบอกฉีดยา (CanP) กลุ่มที่ 3 ใช้สกรูสำหรับกระดูกทึบขนาด 3.5 มิลลิเมตรร่วมกับพอลิเมทิลเมทาคริเลตที่ใช้เทคนิคกระบอกฉีดยา (CorP) และกลุ่มที่ 4 ใช้สกรูสำหรับกระดูกทึบขนาด 3.5 มิลลิเมตรร่วมกับแผ่นดามกระดูกชนิดเอสโอพี (SOP) ผลการศึกษานี้พบว่า กลุ่ม SOP ต้องใช้จำนวนรอบที่มากที่สุดในการทำให้เกิดการล้มเหลวของอุปกรณ์จากการล้าตัวและมากกว่ากลุ่ม CorP CanP และกลุ่ม MP ตามลำดับจากมากไปน้อย ยิ่งไปกว่านั้นลักษณะการล้มเหลวของอุปกรณ์จากการล้าตัวสามารถบ่งชี้ถึงส่วนที่อ่อนแอที่สุดของอุปกรณ์ยึดดามได้ พบว่า พอลิเมทิลเมทาคริเลตที่ใช้ในลักษณะการปั้นมือ สกรูสำหรับกระดูกฟ่ามขนาด 3.5 มิลลิเมตร พอลิเมทิลเมทาคริเลตที่ใช้เทคนิคกระบอกฉีดยา และสกรูสำหรับกระดูกทึบขนาด 3.5 มิลลิเมตร เป็นส่วนที่อ่อนแอที่สุดของอุปกรณ์ยึดดามในกลุ่ม MP CanP CorP และ SOP ตามลำดับ และสามารถสรุปผลการศึกษาจากคุณสมบัติเชิงการล้าตัวของอุปกรณ์ทั้ง 4 ชนิดนี้ได้ว่า แผ่นดามกระดูกสันหลังชนิดเอสโอพีอาจเป็นอุปกรณ์การรักษามาตรฐานในสุนัขที่มีภาวะกระดูกสันหลังหักและเคลื่อน

ภาควิชา ศัลยศาสตร์ ลายมือชื่อนิสิต .....

สาขาวิชา ศัลยศาสตร์ทางสัตวแพทย์ ลายมือชื่อ อ.ที่ปรึกษาหลัก .....

ปีการศึกษา 2560

5875318131 : MAJOR VETERINARY SURGERY
KEYWORDS: CYCLES TO FAILURE / FAILURE MODE / POLYMETHYLMETHACRYLATE / STRESS CONCENTRATION / SOP PLATE

MINGRATH MEKAVICHAI: Fatigue study of cancellous and cortical stainless steel screws used with polymethymethacrylate and the SOP plate system for the immobilisation of vertebral fracture and luxation in canine cadavers. ADVISOR: ASST. PROF. KUMPANART SOONTORNVIPART, D. V. M. , Ph. D. , D.T.B.V.S., 67 pp.

Globally, vertebral fracture and luxation (VFL) are one of the most common neurological injuries in dogs and cats. The standard care for vertebral body stabilisation of canine VFL are screws with polymethylmethacrylate (PMMA) and the string of pearls (SOP) plate system fixation. The VFL with implants are usually exposed to force in a repetitive or cyclic loading fashion. Indeed, stress on the implant cyclically at a load significantly less than its ultimate tensile strength can cause fatigue failure, one of the major causes of implant breakage. This study aims to compare the failure mode of four different implants using a specifically designed fatigue testing machine. The four different implants were constructed as follows: 3.5 mm cancellous screw with manually applied PMMA (MP), 3.5 mm cancellous screws with syringe application of PMMA (CanP), 3.5 mm cortical screws with syringe application of PMMA (CorP) and 3.5 mm cortical screws with a SOP plate (SOP). The results revealed that the SOP group tolerated the most cycles before failure, followed by the CorP, CanP and MP groups repectively. The point of weakness, as defined by the failure mode, occurred in the middle of the PMMA bridge, 3.5 mm cancellous screw neck, PMMA at the screw neck position and 3.5 mm cortical screw in MP, CanP, CorP and SOP groups respectively. In conclusion, based on fatigue properties of the four implants tested in this study, the SOP plate is recommended as a standard fixation device for VFL in dogs.

Department:	Veterinary Surgery	Student's Signature	.....
Field of Study:	Veterinary Surgery	Advisor's Signature	.....
Academic Year:	2017		

ACKNOWLEDGEMENTS

This research is supported by the 90th Anniversary of Chulalongkorn University, Rachadapisek Sompote Fund. The scholarship from Graduate school, Chulalongkorn University to commemorate the 72nd anniversary of his Majesty King Bhumibala Aduladeja is gratefully acknowledged.

I would like to express my deepest thankful to my dearest thesis advisor, Asst. Prof. Dr. Kumpanart Soontornvipart, for his greatest dedication, invaluable advisement, sincerest and warmest encouragement throughout many years. I am truly appreciated her devotion, patience and kindness from all my heart.

I am heartedly appreciated to all my thesis committee (Assist. Prof. Dr. Sumit Durongphongtorn, Prof. Dr. Marissak Kalpravidh, Assoc. Prof. Dr. Chanin Kalpravidh and Dr. Pichanun Linharattanaruksa) for their great helpful and insightful comments to fulfill my thesis.

I am wholeheartedly thanks you to all clinician, staffs of Surgery Clinic Small Animal Teaching Hospital as well as my graduated colleague of Faculty of Engineering and Veterinary medicine Chulalongkorn university and other persons whom I have not been mentioned for their kind assistance, friendship and encouragement.

Finally, I would like to express my heartfelt and overwhelming gratitude to my dearest parents and family, for their advisement, caring, endless love, understanding and everlasting support throughout my whole life. Without them, I would not be accomplished my graduation after all.

CONTENTS

Page

THAI ABSTRACT iv

ENGLISH ABSTRACT v

ACKNOWLEDGEMENTS vi

CONTENTS vii

LIST OF FIGURES x

LIST OF TABLES xiii

LIST OF ABBREVIATIONS xiv

CHAPTER I INTRODUCTION 1

CHAPTER II LITERATURE REVIEW 4

2.1 Vertebral Fracture and Luxation (VFL) 4

2.1.2 Biomechanics of VFL 4

2.1.3 Treatment options of VFL 6

2.2 Polymethyl methacrylate (PMMA) 9

2.2.1 General information of PMMA 9

2.2.2 Application method of PMMA 10

2.2.3 PMMA in veterinary field 11

2.3 String of Pearls (SOP) plate 12

2.3.1 General information of SOP plate 12

2.3.2 Mechanical properties of SOP plate 12

2.4 Biomechanics testing of VFL implant 15

2.5 Fatigue analysis 15

CHAPTER III MATERIALS AND METHODS 18

Page

3.1 Specimen Collection and Preparation 18
3.1.1 Inclusion criteria 18
3.1.2 Exclusion criteria 18
3.2 Study Design 19
3.3 Surgical Procedures for Disarticulation and Implant Fixation 19
3.3.1 Cancellous screws with manually applied PMMA (MP) group 20
3.3.2 Cancellous screws with syringe application PMMA (CanP) group 20
3.3.3 Cortical screws with syringe application PMMA (CorP) group 21
3.3.4 Cortical screws with SOP plate (SOP) group 21
3.4 The specific designed fatigue testing machine (FTM) 22
3.4.1 Component 22
3.4.2 Machine assembly 23
3.5 Biomechanical testing 33
3.6 Failure mode analysis 34
3.7 Statistical analysis 36
3.8 Correlation study 36
CHAPTER IV RESULTS 37
4.1 Animal 37
4.2 Building fatigue testing machine (FTM) 38
4.2.1 To calculate efficiency of the electric motor 38
4.2.2 To calculate length of the lever arm 39
4.2.3 Specification of this FTM 40
4.2.4 Fatigue testing machine (FTM) application 41

Page

4.3 Fatigue testing analysis 42
4.3.1 Cycles to failure (Fatigue life).....42
4.3.2 Failure mode.....45
4.4 Correlation study.....50
CHAPTER V DISCUSSION and CONCLUSION.....53
Advantages of the study 59
Limitation of the study.....59
Conclusion.....60
Suggestion.....60
REFERENCES.....61
VITA.....67

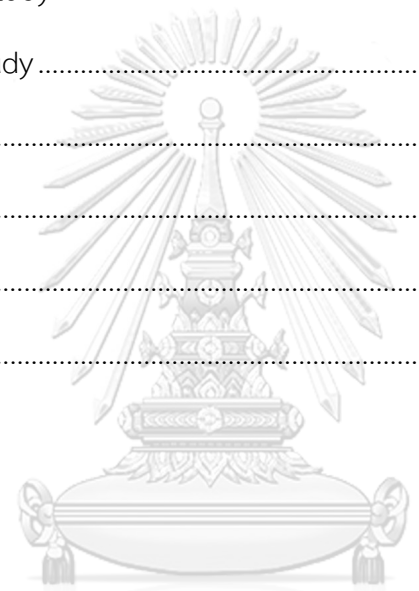

LIST OF FIGURES

Figure 1 Free body diagrams presentation the equilibrium of forces and moments in the cervical, the thoracic and the lumbar spine in a dog 5

Figure 2 Screws was inserted in vertebral body of VFL case before molding PMMA 7

Figure 3 Radiograph of cancellous screw with PMMA in VFL case after application7

Figure 4 Refobacin® PMMA 8

Figure 5 The liquid MMA monomer and a powered MMA-styrene co-polymer 8

Figure 6 SOP plate was inserted in VFL case 13

Figure 7 3.5 millimeters SOP plate system 13

Figure 8 Cross section of string of pearls plate locking system 14

Figure 9 Radiograph of SOP plate system in VFL case after application 14

Figure 10 Nomenclature in cyclic stress testing 17

Figure 11 Before and After putting PMMA into plastic cylinder shape mold.....21

Figure 12 Rotating generator part 23

Figure 13 Electric motor before and after inserting the coupling 24

Figure 14 Axle shaft with 3 flats 24

Figure 15 Eccentric piece 25

Figure 16 Bearing with set screws to lock with the axle shaft flat 25

Figure 17 Conical wedge before and after lathe turning 26

Figure 18 Loading unit before inserting weight 26

Figure 19 Lever arm that made from three iron bars 27

Figure 20 Center punching on the iron bar and center drilling on the iron bar 27

Figure 21 Welding all iron bars, conical wedge and loading unit together 28

Figure 22 Both sides of the pivot axle were connected to both bearings.....28

Figure 23 Specimen fixator with 4 mm pins 29

Figure 24 T-nut with set screw and Tabbed bracket 29

Figure 25 Overall frame.....30

Figure 26 After assembling all part together with frame.....30

Figure 27 Arduino Nano.....31

Figure 28 16x2 Digital LCD 31

Figure 29 IR sensor.....32

Figure 30 Eight kilograms iron rod.....33

Figure 31 Video camera.....34

Figure 32 Stress's nomenclature of various testing frequency.....40

Figure 33 Mean ± SD of cycles to failure withstood by each implant group 43

Figure 34 Cracking formation and propagation in MP group 46

Figure 35 CanP construction failure occurred through the screw neck.....46

Figure 36 Screw hole in CanP construction was markedly dilated.....47

Figure 37 CorP construction failure occurred through PMMA bridges.....47

Figure 38 In the CorP group, cracking formation and propagation along PMMA bridge around the screw neck after testing fatigue failure 48

Figure 39 Screw hole in the CorP construction were dilated 48

Figure 40 In the SOP group, construction failure occurred through the screw neck.....49

Figure 41 In the SOP group, crack formation fissure around the screw neck.....49

Figure 42 Screw hole of SOP group which was not dilated after fatigue testing....50

Figure 43 Regression and correlation between cycles to failure (Y) and cadaveric body weight (X) in the MP group 51

Figure 44 Regression and correlation between cycles to failure (Y) and cadaveric body weight (X) in the CanP group.....51

Figure 45 Regression and correlation between cycles to failure (Y) and cadaveric body weight (X) in the CorP group.....52

Figure 46 Regression and correlation between cycles to failure (Y) and cadaveric body weight (X) in the SOP group.....52

LIST OF TABLES

Table 1 Mean ± SD of body weight and age of canine cadavers.....37

Table 2 Individual data and mean ± SD of cycles to failure (cycles) of each implant group.....44

Table 3 Homogeneity of bridging and bone anchoring compartment of all stabilization construction in this study 57

LIST OF ABBREVIATIONS

CanP	=	3.5 millimeters stainless-steel cancellous screw with syringe technique application PMMA group
cm	=	centimeters
CorP	=	3.5 millimeters stainless-steel cortical screw with syringe technique application PMMA group
CTF	=	cycles to failure
FM	=	failure mode
fps	=	frames per second
FTM	=	fatigue testing machine
HV	=	high viscosity
IR	=	infrared
rpm	=	round per minute
kg	=	kilograms
L	=	lumbar vertebrae
LV	=	low viscosity
m	=	meters
mm	=	millimeters
MP	=	3.5 millimeters stainless-steel cancellous screw with manual application PMMA group
MPa	=	Megapascal
N	=	newton
NM	=	newton meters
PMMA	=	polymethylmethacrylate
S	=	stress
SOP	=	String of Pearls plate
SOP group	=	3.5 millimeters stainless-steel cortical screw with SOP plate group
VFL	=	vertebral fracture and luxation

CHAPTER I

INTRODUCTION

Importance and Rationale

Vertebral fracture and luxation (VFL) are one of the most common neurological injuries in dogs and cats globally (Bruce et al., 2008; Jeffery, 2010). In general, neurological disorders affect quality of dog's life. Moreover, the disorders cause severe pain and functional deficit of many parts of the body such as walking abnormality. VFL occur because of excessive force affecting each segmental spinal column unit which are both bony and soft tissue structure. These structures are constantly subject to external forces including dorsoventral and lateral bending, torsion, shear and axial loading. Furthermore, massive overloading via one or more of these forces causes catastrophic failure of the spinal column, often in the form of VFL (Weh, 2011). Regarding the dog with posterior paralysis, the main forces that effect to vertebral column are dorsoventral bending and lateral bending. Ordinarily, VFL are often the consequence from vehicular injury, which lumbar vertebrae are the most common area effected in dogs (39%) (Feeney and Oliver, 1980). Lumbar VFL cause severe clinical outcome such as both hindlimbs paralysis. For treating VFL cases, procedures can be broadly divided into conservative and surgical means depended on the condition of the patient (Shores, 1992). In case of the patient with severe neurological deficit, severe compression of spinal cord or instable spine should be treated with surgical procedure. The purpose of surgical treatment is reduction of fracture or luxation, decompression of the spinal cord, and rigid stabilization of the vertebral column. A range of methods to fix the vertebral column includes vertebral body plating, external splinting, spinous process plating, Lubra plates, pins or screws with polymethylmethacrylate (PMMA), external skeletal fixation, modified segmental fixation, and tension band technique (Lumb and Brasmer, 1970; Shores et al., 1989; Bruecker, 1996; Voss and Montavon, 2004; Wheeler et al., 2007; Krauss et al., 2012). Currently, the gold standard immobilization method for VFL cases is screws (or pins) with PMMA fixation because this method is practical for clinical application, and provide sufficient rigid stabilization

(Blass and Iii, 1984; Bruecker and Seim, 1992; Aikawa et al., 2007; Jeffery, 2010). In recent years, many studies have been done to prove the stability of screws (or pins) with PMMA implants. These studies mainly tested the strength and the stiffness of implant using single cycle four-point bending model. Garcia et al. (1994) reported that screws (or pins) with PMMA implants gave the greatest strength and rigidity in VFL fixative dogs. In addition, Zotti et al. (2011) studied the maximum force that each implant could resist (single cycle) in four-point bending fashion.

The String of Pearls (SOP) plate system, one of the methods to treat VFL patients, was designed to serve as a locking plate system for the veterinary and human orthopedic community. As with all locking plate systems, the SOP can be assumed mechanically as internal – external fixators. The SOP contains of a series of cylindrical units and spherical components that are made of stainless-steel. There are three assorted sizes which accommodate 3.5 mm, 2.7 mm and 2.0 mm cortical stainless-steel screws (Cronier et al., 2010).

Naturally, after stabilizing VFL with implants, the force that reacts to the implant usually in a repetitive or cyclic loading fashion. So, a significant characteristic of any fracture implant is its fatigue characteristics as it is exposed to cyclic load as the race among fracture healing and implant failure arises (Zand et al., 1983). Fatigue failure is one of the major causes of implant breaking. In human medicine, the fatigue failure of the implant is very important assumption by many studies (Graham et al., 2000; Arora et al., 2013; Ajaxon and Persson, 2014). In addition, the weakest point of PMMA was well established. Fatigue limit or endurance limit are used to describe the material's property. Therefore, these values are used in comparison of fatigue property in PMMA with different implants. Fatigue limit is the highest stress that material can tolerate for an infinite number of cycles (more than 10^6 cycle loading) without breaking (Saha and Pal, 1984). British stainless-steel association reported that fatigue limit of 316L stainless-steel was 270 MPa (megapascal), while fatigue limit of PMMA was only 8.8 MPa which was significantly lower than 316L stainless-steel. Thus, in the fatigue property point of view, SOP plate might be the standard fixation device instead of screws (or pins) with PMMA implants. However, there were no researches that studied about the fatigue property of screws (or pins) with PMMA in canine vertebral model.

Therefore, the present study focused on fatigue property, by means of comparing cycles to failure, from fatigue testing, of two different fixation methods which are stainless-steel screws with PMMA and SOP plates in canine cadaveric VFL models.

The aims of this study were to determine number of cycles to cause failure from fatigue testing of screws with PMMA when compared with SOP plate in canine cadaveric VFL models, and to investigate the difference between type of screws and application methods of PMMA construction. We hypothesized that stainless-steel screws with SOP plate (pure stainless-steel construction) would tolerate more cycles to failure (CTF) from fatigue testing than stainless-steel screws with PMMA (mixed PMMA and stainless-steel construction). PMMA from the application technique using cement syringe method would tolerate more cycles to failure than manually applied method, and the cortical screw would tolerate more cycles to failure than the cancellous screw of the same size.

CHAPTER II

LITERATURE REVIEW

2.1 Vertebral Fracture and Luxation (VFL)

2.1.1 General information

The major cause of neurological injury in dogs and cats is resulted from vertebral fracture and luxation (VFL). VFL are often the consequence from vehicular injury. Other occasional causes of injury include animal attacks or falling from a height (Bruce et al., 2008; Jeffery, 2010). VFL makes up 6% of all feline spinal cord disorders (Marioni-Henry et al., 2004). And 7% of all neurological disorders in dogs (Fluehmann et al., 2006). Feeney and Oliver (1980) studied about the radiographic variations of VFL between dogs and cats. They found that the lumbar area was most commonly affected in dogs (39%) and the sacrocaudal segment in cats (46%). According to Carberry et al. (1989) studies, they found that the most common level of VFL has been reported at the terminal area between the mobile and immobile sections of the vertebral column, for instance the thoracolumbar and lumbosacral junctions. These areas increased the incidence of fracture-luxation because the stress concentration effect. Moreover, the severity and level of injury depend on the animal's posture on impact, the types of force transmitted, the area of impact and inherent strengths and weaknesses of the vertebral column (Bagley, 2000).

2.1.2 Biomechanics of VFL

Many difference types of VFL can occur reliant on the mixing of loading forces applied and the location along the spine. Forces can be alienated into axial loading, flexion and extension, and rotation with each creating a different type of vertebral column injuries (Olby, 2015). For instance, for the head and neck of a dog to stay at rest, the state of equilibrium is that the resultant of forces and moments is zero (Figure 1). By way of spine segments do not resist extensive bending moments themselves, equilibrium must be provided by forces from dorsal muscles or ligaments. In fact, the cervical spine works similar a hoist, with supports that are individually

loaded by tension (the muscles and the nuchal ligament) or compression (the vertebrae). A parallel study can be performed for the thoracolumbar spine. The portion of the trunk with a negative moment (Figure 1) has the propensity to extend because of the gravitational forces. In effect, the ventral part of the trunk is stretched under its own weight, whereas the dorsal part is compressed. This compressive force is resisted by the spine, while stretching is mitigated by the ventral muscles, predominantly effectively by the rectus abdominis muscle, which of all muscles has the longest lever arm to the spine, and the passive tensile band linea alba (Nickel, 1986).

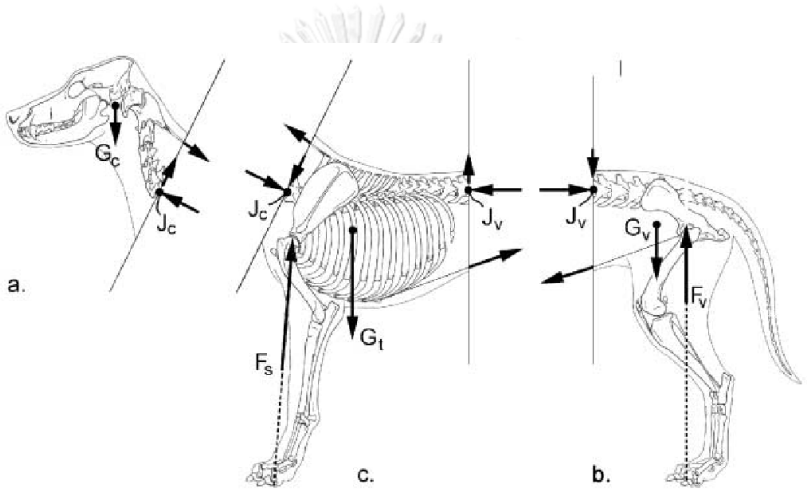

Figure 1 Free body diagrams presentation the equilibrium of forces and moments in the cervical, the thoracic and the lumbar spine in a dog. (a) The weight of head and neck (G_c) presents a flexing moment around cervical joint J_c. To avoid this portion from drooping, a tensile force T_c is required, which is largely provided by a passive structure called nuchal ligament. Equilibrium of forces is sustained by a compressive force on the vertebral body F_b and a facet joint force F_f. (b) The lumbar spine is loaded by a flexion moment owing to pelvic force F_p and a gravitational force G_l, which is counterbalanced by a tensile force T_l and a lumbar compression force F_b in joint J_l. The resultant of F_b and facet joint force F_f is equal and opposite to the resultant of F_p, G_l and T_l. (c) The thoracic spine is loaded by a shoulder force F_s, a gravitational force G_t, tensile forces T_c and T_l, and the vertebral loads F_b and F_f in the cervical and lumbar joints J_c and J_l (Smit, 2002).

2.1.3 Treatment options of VFL

The main problems of VFL are pain and neurologic deficit. Compression and contusion of neural tissue cause neurologic deficit. On the other hand, pain arise from neural compression or direct mechanical injury and mesenchymal tissues instability (Jeffery, 2010). Furthermore, prolong compression of the spinal cord parenchyma or the nerve roots causes demyelination, progressive axonal injury, and neuronal and axonal destruction (Olby, 2010). So, the purpose of treatment is saving of function in surviving neural tissue, which sometime requires decompression and stabilization by surgery to avoid further trauma, together with physiotherapy and rehabilitation to recovery damaged tissue (Jeffery, 2010).

Treatment procedure selected depends on the signalment, injury type, neurological condition, and surgeon preference. And treatment procedure can be broadly divided into conservative and surgical options. For cases that have minimal neurologic deficits, function can recover sufficiently with conservative therapy alone, because of inherent stability of the vertebral column to forestall further trauma to the nervous system. Conservative treatment regularly involves external immobilization in the manner of splints and bandages, cage confinement, exercise restriction, and steroid administration. Conversely, patient with severe neurological deficit, severe compression of spinal cord or instable spine should be treated with surgical procedures (Shores, 1992).

The purpose of surgical treatment is reduction of fracture or luxation, decompression of the spinal cord and rigid stabilization of the vertebral column. A range of methods how to stabilize vertebral column including vertebral body plating, external splinting, spinous process plating, Lubra plates, pins or screws with polymethylmethacrylate (PMMA), external skeletal fixation, modified segmental fixation and tension band technique (Lumb and Brasmer, 1970; Shores et al., 1989; Bruecker, 1996; Voss and Montavon, 2004; Wheeler et al., 2007; Krauss et al., 2012). Pins or screws with PMMA have been commonly used over the past ten-year because of the potency and adjustability of this technique for spinal stabilization (Rouse and Miller, 1975; Blass and Iii, 1984; Jeffery, 2010). So, Pins (or screws) with PMMA fixation

abides a gold standard for vertebral body stabilization of the canine thoracolumbar spine (Blass and Iii, 1984; Bruecker and Seim, 1992; Aikawa et al., 2007; Jeffery, 2010). Furthermore, Screws (or Pins) with PMMA implants provides rigid stabilization to all part of the vertebral column in any sized dog and cat (Blass and Iii, 1984; Jeffery, 2010).

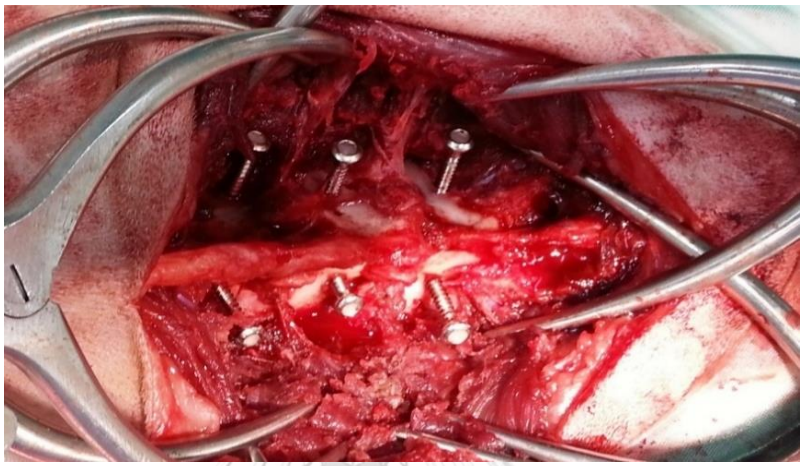

Figure 2 Screws was inserted in vertebral body of VFL case before molding PMMA above screws head.

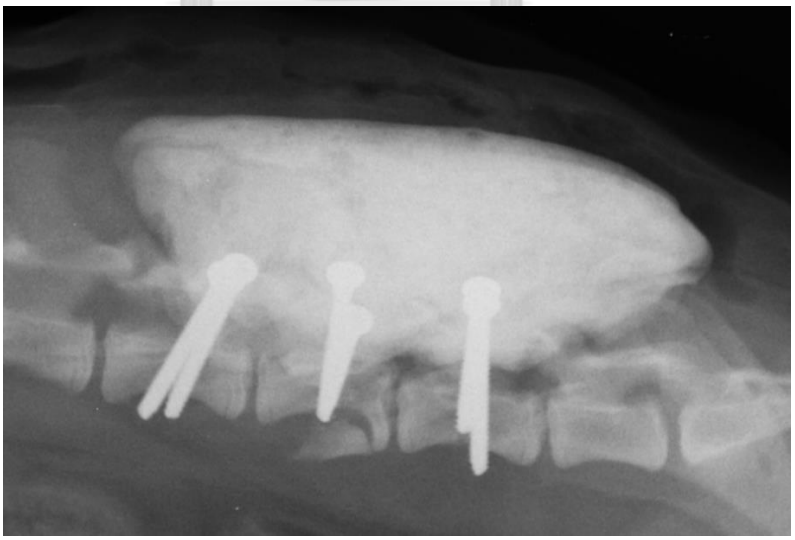

Figure 3 Radiograph of cancellous screw with PMMA in VFL case after application

Figure 4 Refobacin® PMMA

Figure 5 The liquid MMA monomer and a powered MMA-styrene co-polymer.

2.2 Polymethyl methacrylate (PMMA)

2.2.1 General information of PMMA

Polymethyl methacrylate (PMMA), is regularly known as bone cement, and is broadly used for implant fixation in various orthopedic and trauma surgery. PMMA acts as a space-filler that makes a tight space which holds the implant against the bone. Bone cements have no intrinsic adhesive properties. Other forms of commercially available bone cement like calcium phosphate cements (CPCs) and Glass polyalkenoate (ionomer) cements (GPCs) are successfully used in a variety of orthopedic and dental applications (Vaishya et al., 2013). PMMA is an acrylic polymer that is formed by mixing two sterile components, a liquid MMA monomer and a powered MMA-styrene co-polymer (Figure 5). When the two components are mixed, the liquid monomer polymerizes around the pre-polymerized powder particles to form hardened PMMA. In the course, heat is created, due to an exothermic reaction. Exposure to light or elevated temperatures can cause early polymerization of the liquid component. The curing process is divided into 4 phases mixing, sticky, working and hardening. The mixing can be done by hand or with the aid of centrifugation or vacuum technologies. Bone cements are heat sensitive. Any increase or decrease in temperature affects the handling characteristics and setting period of the cement (Eveleigh, 2001). PMMA can be divided into various type of viscosity. Viscosity describes the PMMA struggle to flow. PMMA is classified by which state it remains in the longest. Typically, a low (LV) or high (HV) viscosity cement stays for a long time in one state. As, a LV cement spends more of its working time in a low viscosity state. Thus, if a high viscosity state is desired, the working time may be too short for the application time needed. On the other hand, HV cements are thick immediately after mixing and can only be used in that high viscosity state. High viscosity cements are occasionally pre-chilled for use with mixing systems for easier mixing and prolonged working phase. This will also increase the setting time. The relative humidity might also effect the handling properties. That is the reason why the working time and setting time of the cement might vary in winter and summer (Mjoberg et al., 1987).

2.2.2 Application method of PMMA

There are various methods exist for the application of PMMA.

Manually applied

All PMMA can be applied digitally. The cement is mixed thoroughly but carefully to minimize the entrapment of air. Once dough is formed the surgeon should wait until the cement no longer adheres to the glove and the surface has become dull as opposed to shiny. The cement can then be taken into gloved hands and kneaded thoroughly. Importantly, this stage will occur at various times for different cement types. The time of cement application and prosthesis insertion is at the discretion of the surgeon and will depend upon the surgical procedure used. In general, implant insertion should be delayed until the cement has developed a sufficient degree of viscosity to resist excessive displacement by the implant. However, implant insertion should not be delayed such that there is a risk that the procedure cannot be completed due to cement hardening. Following introduction, the implant must be firmly held in position to avoid movement and pressurization must be maintained until the cement finally hardens. Excess bone cement must be removed before the cement has completely hardened (Eveleigh, 2001).

Syringe application

PMMA may be applied using a suitable cement gun and syringe. The surgeon should use their experience to judge when the cement has reached an appropriate viscosity to be extruded. This will not occur until after the cement has formed dough. A small amount of cement should be extruded from the syringe and visually assessed to ensure that the surface of the cement appears dull and excessive flow under gravity has ceased. Once the cavity is filled it is advisable that adequate pressurization is applied and maintained up to the point of hardening (Heisel et al., 2003).

Different methods for PMMA application cause change porosity inside the cement. Porosity is air entrapped in bone cement, which can lead to mechanical failure. Reduction in porosity increases fatigue strength. so, if a surgeon waits too long to apply a high viscosity cement, laminations or folds can occur in the cement mantle. A lamination could reduce cement strength (Oh et al., 1983).

2.2.3 PMMA in veterinary field

In veterinary field, screw with PMMA was used in various of fashion. Garcia et al. (1994) recommended that using 3.5 mm cortical stainless-steel screws in VFL case has no significantly difference to 3.2 mm diameter pin. But in human medicine, there recommended to use cancellous screw in VFL cases because of loosening of screws due to poor fixation in vertebrae (Arbi, 1998). Gordon-Evans (2015) reported the most complication of using PMMA in VFL cases is PMMA fracture. PMMA application was always used for VFL cases in Veterinary medicine. Whereas, used for arthroplasty in human medicine. So, the most common complication of cemented (PMMA) arthroplasty, one of the surgical fixation of artificial joint, is loosening of the cemented prosthesis due to fracture of PMMA (Khaled et al., 2011; Arora et al., 2013). There had many studies on the fatigue properties of PMMA. Graham et al. (2000) study about effects of sterilization, molecular weight, and mixing method on the fracture and fatigue performance of PMMA. Ajaxon and Persson (2014) studied about compressive fatigue properties of a commercially available acrylic bone cement for vertebroplasty. So, it could be summarized that PMMA still had a weak point in fatigue failure. Fatigue failure of PMMA caused by crack formation that was induced by cyclic loading. And cyclic loading is very important because it can cause fatigue fracture in human lumbar vertebrae (Brinckmann et al., 1988; Graham et al., 2000; Arora et al., 2013; Ajaxon and Persson, 2014).

2.3 String of Pearls (SOP) plate (Figure 7)

2.3.1 General information of SOP plate

String of Pearls (SOP) plate, one of the methods to treat VFL patients. SOP plate was designed to serve as a locking plate system for the veterinary and human orthopedic community. As with all locking plate systems, the SOP can be assumed of mechanically as internal – external fixators. The SOP contains of a series of cylindrical units and spherical components. There are three assorted sizes which accommodate 3.5 mm, 2.7 mm and 2.0 mm cortical stainless-steel screws. Mechanical testing using ASTM standards has proved that the 3.5 SOP is 50% stiffer, and has a bending strength of 16-30% greater than the LCP, DCP, or LC-DCP. Plate pullout force is significantly greater than DCP plates, particularly in flat bones. The SOP be contoured in six degrees of freedom; medial to lateral bending, cranial to caudal bending, and torsion using specially designed bending irons. The plates can be used in pair as they are designed to nest together. The SOP plates accepts standard cortical screws. This greatly reduces cost of implant, and total implant costs are comparable to standard DCP plating. The disadvantage is that standard bone screws have relatively small minor diameters. Screw breakage is a concern if too few screws per bone segment are used. Typically, four screws, either unicortical or bicortical, are recommended. It may be required to add a second SOP plate to accomplish sufficient numbers of screws. The SOP system is firmly a buttress plating system. Fractures that are best treated with dynamic compression should be fixed with DCP systems. The plates are not luted to bone, and as such failure is not typically be screw pullout, rather implant breakage or bone slicing (Ness, 2009).

2.3.2 Mechanical properties of SOP plate

The locking plate acts similar an external fixator but without the weaknesses of an external system not only in the transfixion of the soft tissues, but also in terms of its mechanics and the risk for sepsis. In human medicine, the modification from the conservative nail to the locking nail was a revolution. This is an evolving implant but one that leftovers within the same conceptual framework, spreading its indications.

There are two wide-ranging types of locking plates, fixed-angle locking plates and variable-angle locking plates. In the latter, the screw can be locked with a certain clearance within a cone with an angle on the order of 1—15°. The mechanism locking the screw in the plate also comes in two types. In the first, the screw head is locked in its slot by a threaded locknut. In the second, the screw head is itself threaded and screws into the plate or into an adapted lip (Cronier et al., 2010).

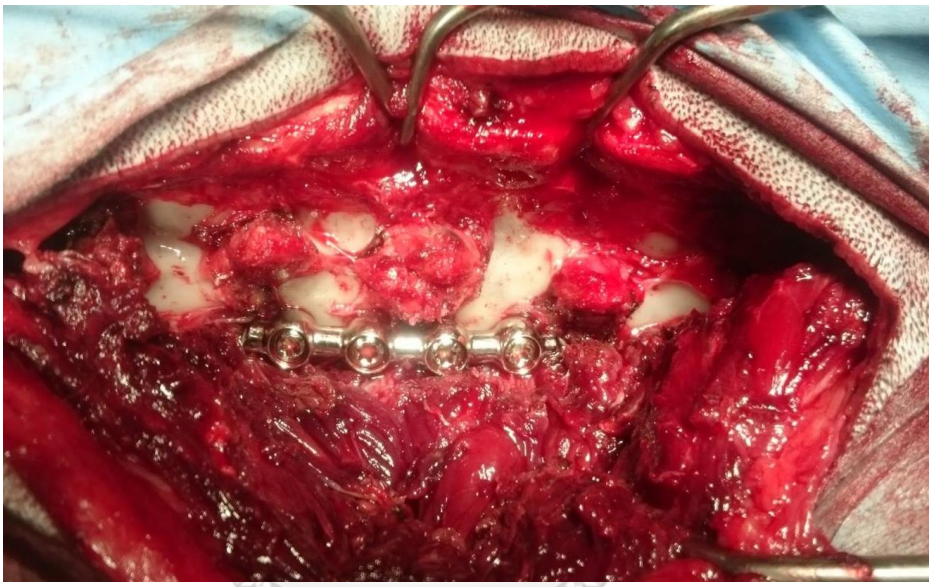

Figure 6 SOP plate was inserted in VFL case.

Figure 7 3.5 millimeters SOP plate system

Figure 8 Cross section of string of pearls plate locking system (Mariscoli, 2014)

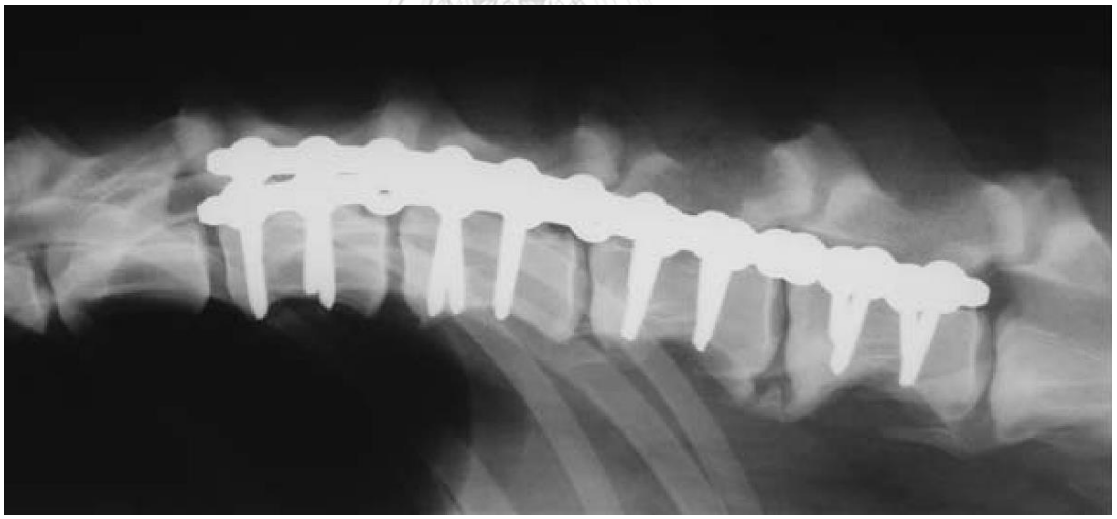

Figure 9 Radiograph of SOP plate system in VFL case after application

2.4 Biomechanics testing of VFL implant

Many studies have been done proofing the stability of screws (or Pins) with PMMA implants. Every study was tested by using four-point-bending model. According to Garcia et al. (1994) studied on the biomechanics of canine VFL fixation using pins or bone screws with PMMA. It was found that screws (or Pins) with PMMA implants had the greatest strength and rigidity. Many literatures profound the tested the stability of screws (or Pins) with PMMA implants in the other point of view. Hall et al. (2015) studied bending strength and stiffness of dog cadaver vertebrae after stabilization of a lumbar VFL using a novel unilateral stabilization technique compared to traditional dorsal stabilization. According to Sturges et al. (2016) which studied about the biomechanical collating of locking compression plate versus positive profile pins and PMMA for stabilization of the canine VFL. Both of studies mention above were also tested by using four-point bending model. This model was tested under the purpose to measure the maximum force that any implants can be resisted (single cycle). Results of studies showed that PMMA is the most resistant implant. So currently, PMMA became the standard of care to treatment VFL.

2.5 Fatigue analysis

As described earlier, all studies emphasized that the bending force in dorsal and lateral bending are the main forces which effect on the vertebral column. It was true that the main function of vertebrae is to withstand bending in the dorsal and lateral direction. But besides the maximum force that implant can be resisted, it also had cyclic loading which effect on vertebral column. The best way to stimulate cyclic loading in vitro called “Fatigue analysis” (Zotti et al., 2011).

Fatigue is the progressive, localized, enduring physical alteration that occurs in materials exposed to fluctuated stresses and strains that might result in fracture subsequently a sufficient number of fluctuations. Fatigue fractures are caused by the simultaneous action of cyclic stress, tensile stress and plastic strain. If any one of these three actions is not existing, fatigue cracking will not initiate and propagate. The cyclic stress starts the crack, the tensile stress produces crack growth (propagation). The

process of fatigue consists of three stages. Initial fatigue damage leading to crack nucleation and crack initiation. Progressive cyclic growth of a crack (crack propagation) until the residual uncracked cross section of a part becomes too weak to withstand the loads imposed. Finally, sudden fracture of the lasting cross section. Fatigue cracking typically results from cyclic stresses that are well beneath the static yield strength of the material. In low-cycle fatigue, though, the stresses also may be above the static yield strength. Fatigue cracks initiate and propagate in areas wherever the strain is most severe. Since most materials contain defects, most fatigue cracks initiate and grow from physical defects. Under the action of cyclic loading, an area of deformation (plastic zone) develops at the defect tip. This region of high deformation develops an initiation site for a fatigue crack. The crack propagates under the applied stress over the material till complete fracture results. On the microscopic scale, the most significant feature of the fatigue process is nucleation of one or more cracks under the influence of reversed stresses that exceed the flow stress, followed by development of cracks at persistent slip bands (Boyer, 1986).

During a fatigue test, the stress cycle usually is maintained constant so that the applied stress conditions can be written $S_m \pm S_a$, where S_m is the static or mean stress, and S_a is the alternating stress, which is equal to half the stress range. Nomenclature to describe test parameters involved in cyclic stress testing are shown in Figure 10. The continual amplitude cyclic loading and is recognized as the Wohler S-N diagram. The S-N approach is still a valuable tool to evaluate fatigue failure of many structures that are exposed to repetitive loading, where the applied stress is under the elastic limit of the material and the number of cycles to failure is large. Once material failure arises under a relatively enormous number of cycles, and stresses and strains are within the elastic range of the material, the failure mechanism is termed high-cycle fatigue. If the magnitude of the fluctuating stress is no longer in the elastic range of the material, significant plastic straining occurs throughout the body and the number of cycles to failure is predictable to be quite short. This failure mechanism is referred to as low-cycle fatigue. Low-cycle fatigue failure, sometimes referred to as the strain-controlled or strain-life (e-N) approach, can no longer be characterized by an S-N curve. Low-cycle fatigue life is typically associated with number of cycles to failure between 100 and

10,000 cycles and for high-cycle fatigue the number is above 10,000 cycles (Farahmand, 1997).

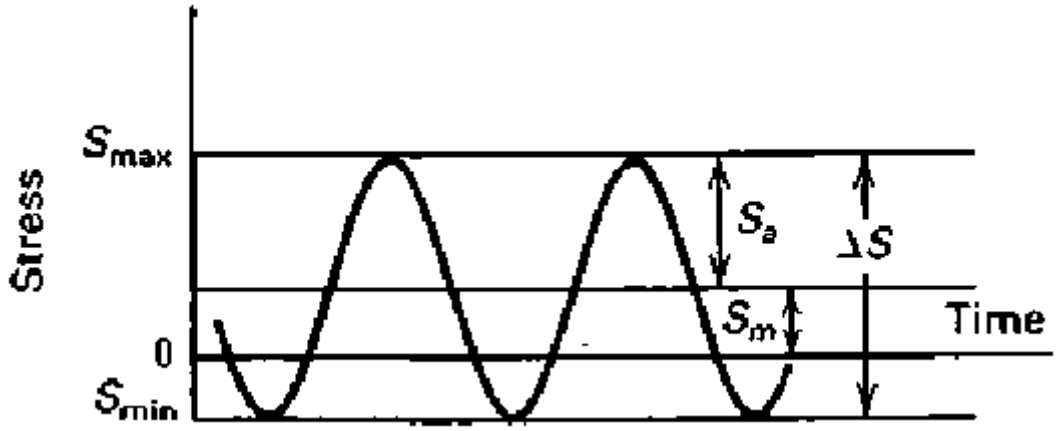

Figure 10 Nomenclature to describe test parameters involved in cyclic stress testing (Boyer, 1986).

While, SOP plate did not a current standard of care. But it had better fatigue property than PMMA. Information that can use to compare fatigue property between material called fatigue limit or endurance limit. Fatigue limit is the highest stress that a material can tolerate for an infinite number of cycles (more than 10^6 cycle loading) without breaking. British stainless-steel association reported that fatigue limit of 316L stainless steel is 270 MPa (megapascal). While fatigue limit of PMMA is 8.8 MPa that a lot lower than 316L stainless steel. So, in the fatigue property point of view, SOP plate might be the standard of care instead of screws (or Pins) with PMMA implants (Saha and Pal, 1984). But no study had been done in canine vertebral model.

CHAPTER III

MATERIALS AND METHODS

3.1 Specimen Collection and Preparation

Lumbar (L1-L6) vertebral column specimens were collected from twenty canine cadavers. The study was performed at the Department of Veterinary Surgery, Faculty of Veterinary Science, Chulalongkorn University. All specimens were assessed skeletal maturity and the absence of vertebral pathology using lateral and dorsoventral radiographs (FCR CAPSULA V VIEW workstation®).

3.1.1 Inclusion criteria

Specimen qualified to be included in the study must meet all inclusion criteria below.

1. Weight between 15-25 kg
2. Mature skeleton
3. Age between 2-10 years old

3.1.2 Exclusion criteria

1. History of vertebral fracture and luxation
2. History of any vertebral column diseases
3. History of neurological problems
4. History of metabolic diseases
5. Vertebral deformity
6. Evidence of bone opacity changing or other pathology

Lumbar vertebrae specimens (L1-L6) were collected from selected canine cadavers. Hypaxial and epaxial muscle, spinal ligaments (supraspinous and interspinous ligaments, and ligamentum flavum), and joint capsules were stored. The tissues were kept moist with 0.9% saline solution during preparation, storage, and testing. Subsequently, specimens were wrapped in saline soaked towels and plastic bags then

stored at -20°C. Specimens were thawed at ambient temperature for 24 hours prior to mechanical testing (Balligand, 2016).

3.2 Study Design

Prospective study

The study was to compare cycles to failure from fatigue testing among 4 groups including;

1) 3.5 mm stainless-steel cancellous screw with manually applied PMMA
2) 3.5 mm stainless-steel cancellous screws with syringe application PMMA
3) 3.5 mm stainless-steel cortical screws with syringe application PMMA
4) 3.5 mm stainless-steel cortical screws with SOP system plate

The fatigue properties in this study are the number of cycles that cause implant failure from cyclic loading forces (cycles to failure) and failure mode. These data were obtained by using specific design fatigue testing machine. The lumbar (L1-L6) vertebral column specimens that collected from twenty canine cadavers were assigned equally to four groups. After disarticulating, all of specimens were assigned equally to one of four fixation groups, five specimens in cancellous stainless-steel screws with manually applied PMMA group, five specimens in cancellous stainless-steel screws with PMMA group, five specimens in cortical screws with PMMA group, and five cadavers in cortical screws with SOP plate group. Body weights of the cadaver were matched among groups.

3.3 Surgical Procedures for Disarticulation and Implant Fixation

Every treatment was performed by only one surgeon. Prior to the experiment, the specimens were thawed at room temperature for 24 hours. 4.0 mm pins were inserted at L1 and L6 vertebral body for fixation with fatigue testing machine (FTM). Then, each spine was disarticulated at the L3-L4 intervertebral disc space by totally

removal of the entire L3-L4 disc (nucleus pulposus and annulus fibrosus excised). The joint facet was sectioned with a scalpel blade number four directed dorsally via a ventral approach through the disc space and canal. All tissues at L3-L4 vertebrae except bone were removed. All specimens must be exposed two landmarks which are an accessory process and base of the transverse process. Finally, the specimen was completely separated into two sections at L3-L4 junction.

3.3.1 Cancellous screws with manually applied PMMA (MP) group

Four 3.5 mm stainless-steel cancellous screws were inserted into both sides of the vertebral bodies of L3 and L4 just above base of the transverse process and below the accessory process; one screw at side of each vertebral body. For each screw, a hole was drilled into the ciscortex with a 2.5 mm drill bit and tapped with a 3.5 mm thread tap. Orientation of the screw was directed away from the spinal canal at an angle 70–80° from the dorsal plane. Moreover, length of screws was estimated based on measurements from pre-fixation lateral radiographs of the vertebral bodies, as well as keeping the distance between the screw and the vertebral body approximately 1 centimeter for filling with PMMA. Luxation was reduced by using towel cramps grasping each side of the articular process. Then, before PMMA was mixed until the paste did not adhere to the instruments or surgical gloves, applying it around screw heads on both sides, connecting all screw heads on the same side.

3.3.2 Cancellous screws with syringe application PMMA (CanP) group

Application of four 3.5 mm stainless-steel cancellous screws were performed as described in the MP group. The luxation of vertebrae was also reduced by using towel cramps grasping each side of the articular process. Subsequently, plastic taken from normal saline bottle was used as a mold of PMMA. Creating a hole for inserting screw through the plastic. Then, suturing the plastic to make a cylinder shape mold for PMMA with a diameter of cylinder shape to 2 centimeters (Figure 11A). Finally, the well mixed PMMA (Refoboacin®) before doughing phase was put into a 10 ml syringe and injected into the plastic cylinder mold (Figure 11B).

3.3.3 Cortical screws with syringe application PMMA (CorP) group

Application of four 3.5 millimeters (mm) stainless steel cortical screws were performed as described in the MP group. The luxation of the vertebrae was reduced by using towel cramps grasping each side of the articular process. PMMA application was also similar to that in the CanP group.

3.3.4 Cortical screws with SOP plate (SOP) group

Specimens undergoing SOP fixation had 2 parallel 3-hole 3.5 mm SOP plates (Orthomed, Halifax, West Yorkshire, UK) applied to both sides of the lateral vertebral body surfaces. Then, plate was placed just above the base of the transverse process and below the accessory process. The middle hole of SOP plate was placed over the intervertebral disc space and the rest holes were placed on the vertebral body. A 2.5 mm drill bit and a plate specific guide (Orthomed, Halifax, West Yorkshire, UK) was used to drill the cis and trans cortex and 3.5 mm tapping was used to create thread only cis cortex. The 3.5 mm non-self-tapping stainless-steel cortical screws were placed bicortical. Length of the screw was estimated based on measurements from pre-fixation lateral radiographs of the vertebral bodies and approximate distance between the screw hole and bone surface. Finally, all specimens were taken radiographs.

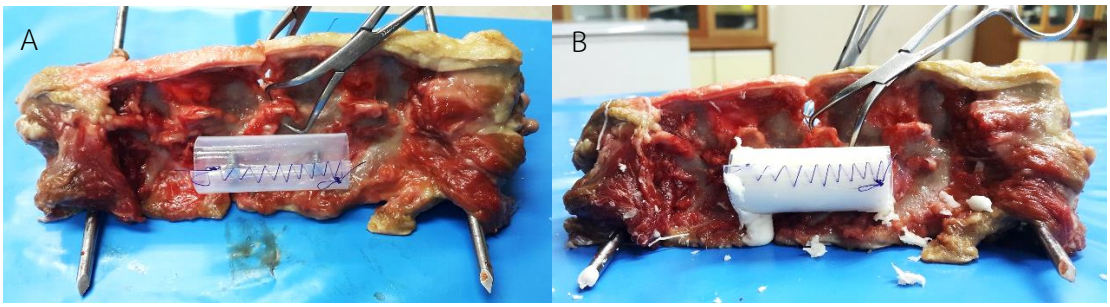

Figure 11 (A) Before and (B) After putting well mixed PMMA into suturing plastic cylinder shape mold

3.4 The specific designed fatigue testing machine (FTM)

3.4.1 Component

1. *Electric motor:* An electric motor was a machine that consumes electrical energy and in turn produce mechanical energy. The electric motor was used as a single-phase AC 25 watt that generated the rotation at 80 rounds per minute.
2. *Frame:* Frame was a main supporting element in the system by bearing all weight of the experimental set up. The force exerted on the system was distributed to the four legs of the frames. The frame was made from alloy steel of good strength and toughness and welded to serve as the support for the full set up. A flat flexible metallic plate was cut and attached to a part of the frame to serve as a seat for the electric motor.
3. *Coupling:* Coupling was a connector between electric motor and axle.
4. *Eccentric piece:* Eccentric piece was connected to the axle. It was used to control the frequency of fatigue testing.
5. *Lever arm:* Lever arm was connected to a rotary disc frequency generator. The force frequency was sent via this lever arm to the loading unit.
6. *Loading unit:* Loading unit was connected to the lever arm. Loading unit controls the force that react to the specimen.
7. *Wedge:* Wedge was used as a force concentrator to a certain point.
8. *Fixture:* Custom design fixture was connected to the frame. It was used to fix the specimen while running fatigue testing.
9. *Digital counter:* A 6-digit digital counter was used to record the number of the stress cycles that the specimens had been undergone during the test.
10. *Video camera:* Video camera was used to record 24 hours while running fatigue testing machine. Data from video camera provided timing and characteristic of failure.

3.4.2 Machine assembly

FTM can be divided to 5 major compartments including;

1. Rotating generator
2. Connector between rotating generator part and specimen
3. Specimen's fixator
4. Frame
5. Cycle counter

Figure 12 Rotating generator part

1. Rotating generator part (Figure 12) including:

1.1 Electric motor

After connecting electric motor's circuit to cable and plug, motor shaft was connected to the coupling and leaving another end of the coupling to connect to the axle (Figure 13A). The coupling was a spring version to reduce resistant force that affected to the motor after the specimen already broken (Figure 13B).

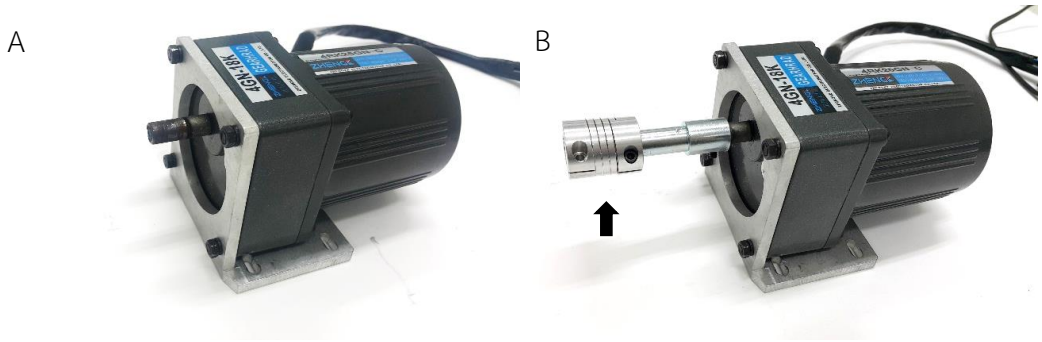

Figure 13 (A) Electric motor before inserting the coupling. (B) Electric motor after inserting the coupling with spring (arrow) to reduce resistant force that affected the motor after specimen already broken.

1.2 Axle shaft

3 flats were made on the axle shaft where the motor's coupling, eccentric piece and bearing with set screws were locked to (Figure 14).

Figure 14 (A) Axle shaft with 3 flats (arrow), (B) flat for set screw

1.3 Eccentric piece (Figure 15)

The eccentric piece hole was dilated for inserting the axle shaft.

Figure 15 Eccentric piece; a screw hole (arrow) for locking to the flat of axle shaft inserted through the axle shaft hole (arrow head).

1.4 Bearing (Figure 16)

After inserting eccentric piece to the axle shaft and connecting the axle shaft to the motor's coupling, the axle shaft was connected to the bearing and all set screws were inserted to lock all components to the shaft (Figure 12).

Figure 16 Bearing with set screws (white arrow) to lock with the axle shaft flat.

2. Connector part (Figure 22) including:

2.1 Conical wedge (Figure 17)

Conical wedge was made from iron rod (Figure 17A) and lathe turning 85 mm iron rod (Figure 17B).

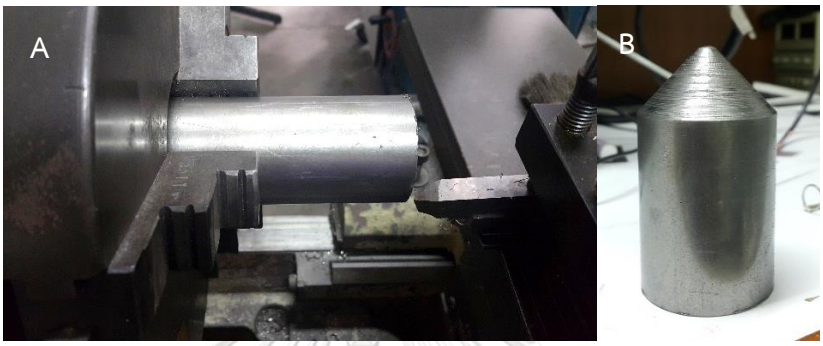

Figure 17 Conical wedge (A) before and (B) after lathe turning.

2.2 Loading unit (Figure 18)

Loading unit was made from aluminum sheet.

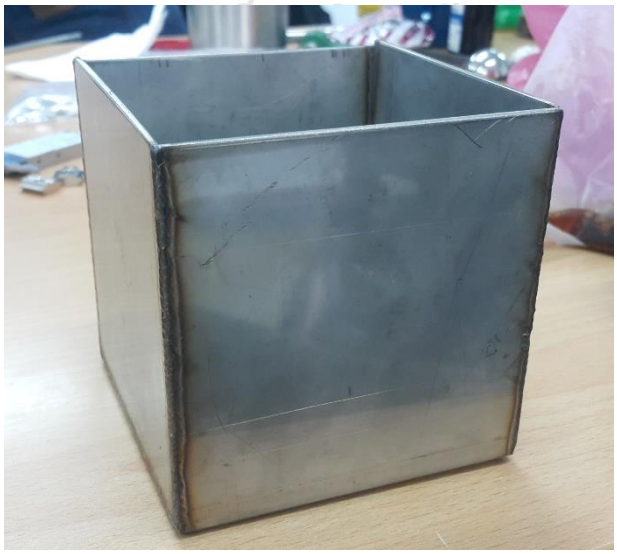

Figure 18 Loading unit before inserting weight.

2.3 Lever arm (Figure 19)

Lever arm was made from three iron bars (length 400 mm). Prior to making a hole on the iron bar, center punching and center drilling were performed before making the pivot axle's hole (Figure 20).

Figure 19 Lever arm that made from three iron bars

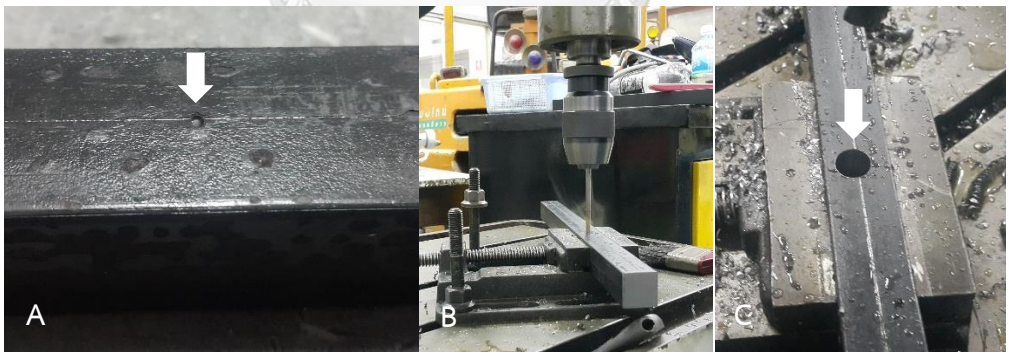

Figure 20 (A) Center punching on the iron bar (arrow), (B) Center drilling on the iron bar, (C) Pivot axle's hole on the iron bar (arrow).

2.4 Pivot axle

Flats were made at both ends of the Pivot axle for locking with both bearing. Pivot axle was put into the pivot axle's hole on the lever arm. Then, all of iron bars were welded with conical wedge and loading unit (Figure 21).

Figure 21 Welding all iron bars, conical wedge and loading unit together

2.5 Bearing (Figure 22)

Bearings were connected to both sides of the pivot axle symmetrically.

Figure 22 Both sides of the pivot axle were connected to both bearings

3. Specimen fixator (Figure 23)

Specimen fixator was made from aluminum profile (AP). AP inside the T-slot was drilled with a 4 mm drill bit to make a hole for 4 mm pin connected to L1 and L6 of specimen. Then, each AP was connected to each other via T-nut (Figure 24A) and tabbed bracket (Figure 24B).

Figure 23 Specimen fixator with 4 mm pins

Figure 24 (A) T-nut with set screw, (B) Tabbed bracket, (C) Tabbed bracket after inserting T-nut

4. Frame (Figure 25)

Frame was made from AP to be a scaffolding of FTM. All AP were connected to T-nut and tabbed bracket. After finishing frame assembling, rotating generator part was connected to the connector part and specimen fixator part on the AP frame (Figure 26). Then, height and length of FTM was adjusted to match with specimen.

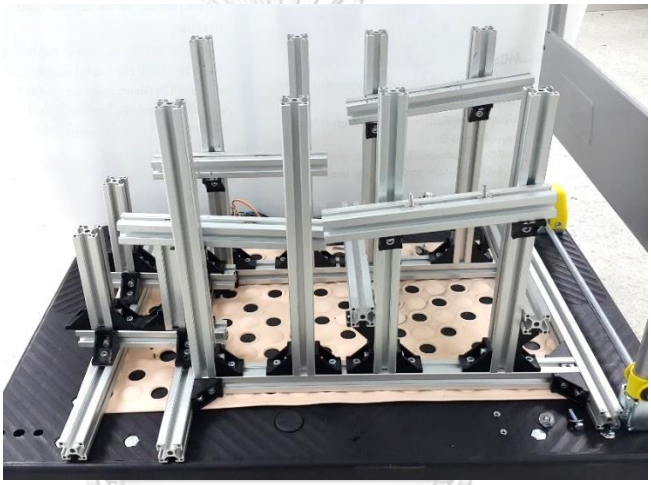

Figure 25 Overall frame

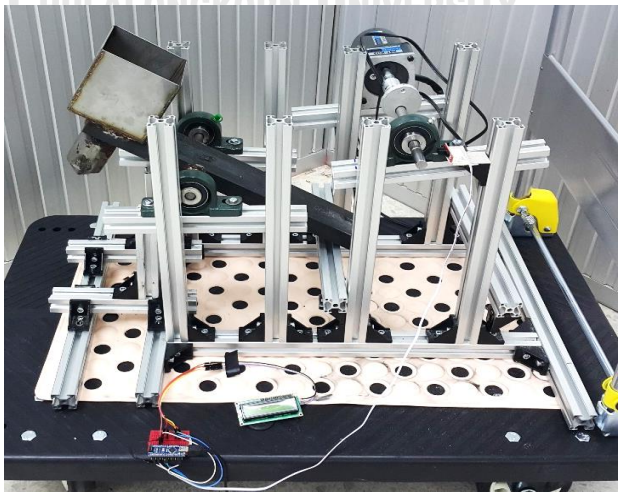

Figure 26 After assembling all part together with frame

5. Cycle counter

Cycle counter includes 3 compartments

5.1 Arduino Nano (Figure 27)

Arduino Nano was used as a main controller. Coding Arduino Nano with Arduino Software to command the infrared sensors to count and display on LCD screen.

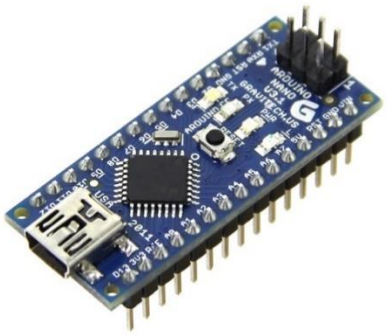

Figure 27 Arduino Nano

5.2 16x2 Digital LCD (Figure 28)

16x2 Digital LCD was connected to Arduino Nano. Then, 16x2 Digital LCD displayed number of the cycle.

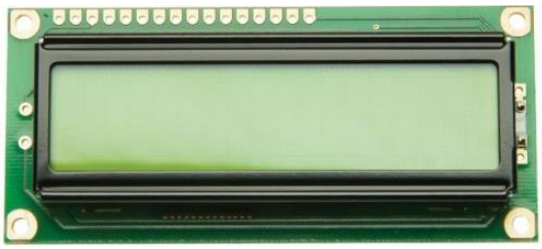

Figure 28 16x2 Digital LCD

5.3 Infrared (IR) sensor module

IR sensor was connected with and sent signal through the Arduino Nano when something interrupted the IR between sensors. The IR sensor was placed at the back of the axle shaft of motor to count the cycle (Figure 29A).

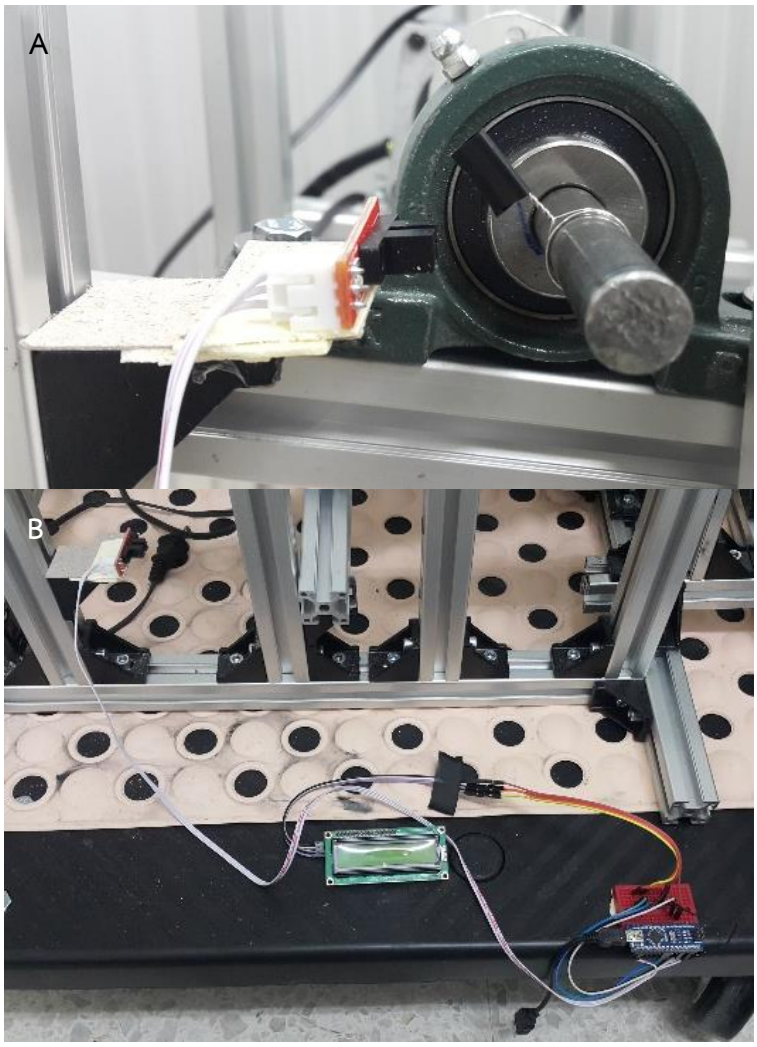

Figure 29 (A) IR sensor was placed just behind the axle shaft. (B) IR sensor connected with Arduino Nano and 16x2 Digital LCD.

3.5 Biomechanical testing

Each specimen was positioned in a fatigue testing machine by inserting 4.0 mm pins fixed at L1 and L6 vertebrae into drilled AP fixator's holes. The length of fixator and height of rotating generator part and connector part were adjusted to the level of the specimen. Finally, all T-nuts and set screws were tightened.

Fatigue tests were performed by applying load to each specimen. The load used in this fatigue test was 40 percent of the average cadaveric bodyweight of 8 kilograms. Load was set by using iron rod weighing eight kilograms (Figure 30). While running fatigue test, specimens were loaded at a constant rate of 1.33 Hz (80 rounds per minute). During testing, sagittal plane video of the specimen was simultaneously recorded using a video camera (AS200V, Sony, Tokyo, Japan) at a rate of 30 frames per sec (fps). Digital cycle counter counted cycle of loading while the test was running. The video was synchronized with number of cycle. The test was run until the implant inside at the specimen were broken and number of cycle was recorded.

Figure 30 Eight kilograms iron rod used as a load in this study.

3.6 Failure mode analysis

During testing, sagittal plane video of the specimen was simultaneously recorded using a video camera (AS200V, Sony, Tokyo, Japan; Figure 31) at a rate of 30 frames per sec (fps). After construction failure, all specimens were taken radiograph. Thus, photos of the implant were taken at the area of implant failure which was recorded as the failure mode of the implant.

Figure 31 Video camera

Conceptual framework

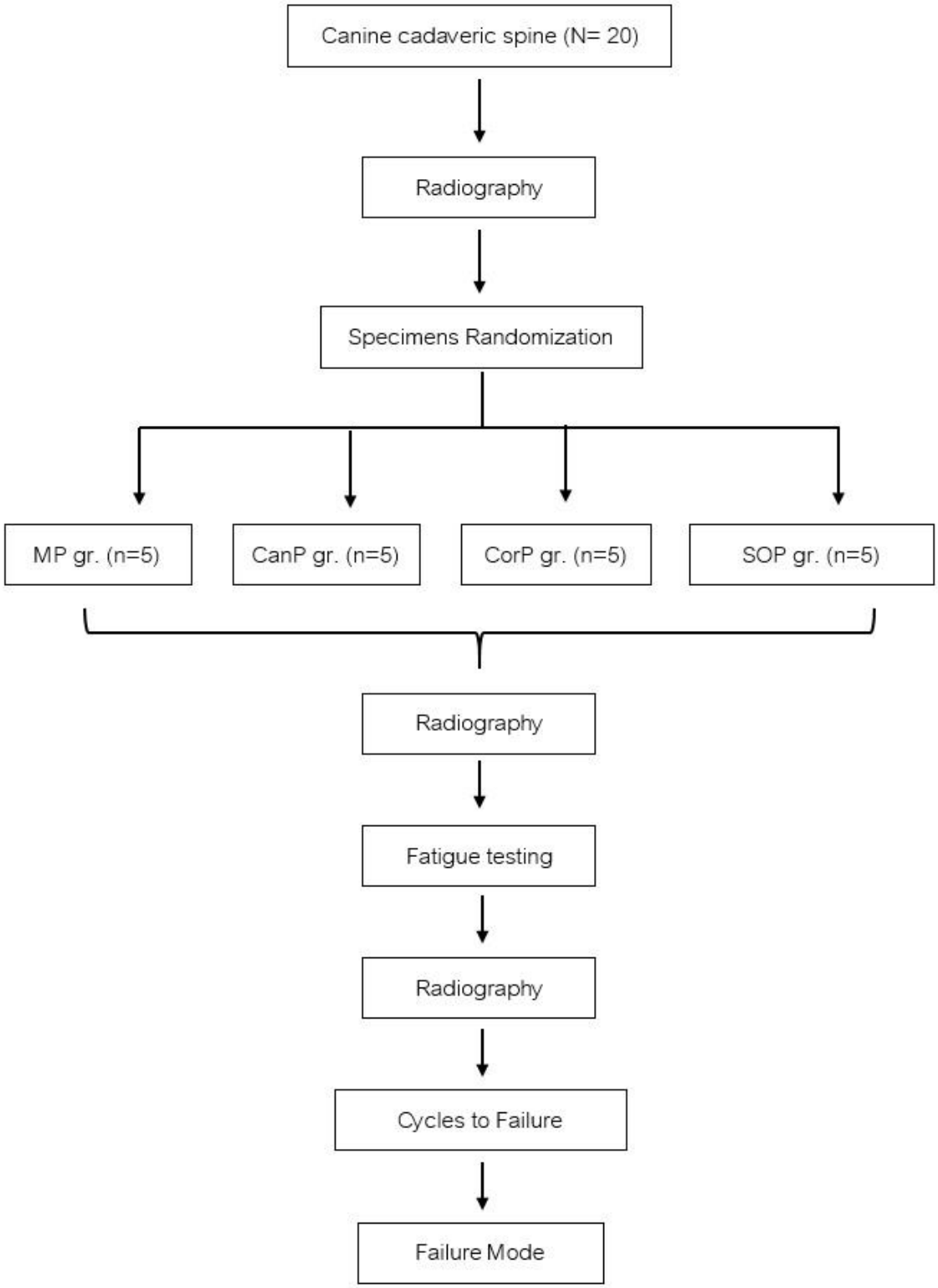

3.7 Statistical analysis

Data was collected using the fatigue testing machine. While testing, the motion while implant failure occurring was recorded in the video camera files. All data were tabulated in Microsoft Excel. Cycles to failure from fatigue testing was analyzed in Microsoft Excel. Data were tested for normality visually using histograms and numerically using the Shapiro-Wilk test. Two-way ANOVA was used to compare the differences of means of number of cycle until fatigue failure occurred. Where ANOVA was indicated a significant difference in a parameter, the Tukey's post hoc test was used to determine which groups differed. P-value < 0.05 is considered statistically significant.

3.8 Correlation study

Pearson's correlation was used to study relationship between cycles to failure and cadaveric body weight of each testing group. Moreover, regression analysis was studied for estimating the relationships among cycles to failure and cadaveric body weight, with significant level at $p<0.05$.

CHAPTER IV

RESULTS

4.1 Animal

Vertebral column specimens were collected from 20 dogs with several dog breeds, including mongrel (n=10), Golden Retriever (n=3), Siberian Husky (n=3), Beagle (n=2) and German Shepherd (n=2). The gender was equal in number of 10 males and 10 females. All specimens were fit the inclusion criteria of weight and age of the animals and skeletal structure. Twenty specimens were divided into 4 groups, including 3.5 mm cancellous screws with manually applied PMMA (MP) group (n=5), 3.5 mm cancellous screws with syringe application PMMA (CanP) group (n=5), 3.5 mm cortical screws with syringe application PMMA (CorP) group (n=5) and 3.5 mm cortical screws with SOP plate (SOP) group (n=5). The bodyweight and age were reported as mean ± SD which were 20.8 ± 3.03 kilograms and 5.4 ± 1.34 years, respectively for the MP group; 19 ± 2.45 kilograms and 5.6 ± 1.81 years, respectively for CanP group; 21 ± 3.67 kilograms and 5.2 ± 1.79 years, respectively for CorP group and 21.2 ± 3.70 kilograms and 5.6 ± 1.82 years, respectively for SOP group (Table 1). The result showed that there was no statistically significant difference of weight and age among groups.

Table 1 Mean ± SD of body weight and age of canine cadavers

	Body weight (kg)	**Age (years)**
MP group (n=5)	20.8 ± 3.0	5.4 ± 1.3
CanP group (n=5)	19.0 ± 2.5	5.6 ± 1.8
CorP group (n=5)	21.0 ± 3.7	5.2 ± 1.8
SOP group (n=5)	21.2 ± 3.7	5.6 ± 1.8

4.2 Building fatigue testing machine (FTM)

This machine uses 25 watts (80 rpm) electric motor as a main power generator. According to the present study design to use eight kilograms load due to a reason that described above, the formula below was used to calculate specification of any part of the machine.

4.2.1 To calculate efficiency of the electric motor

The electric motor potential was calculated from

$$\boldsymbol{T = P/\omega}$$

Where T is Torque (Newton meters). P is power (watts) which is 25 watts from electric motor's specification. **ω** is omega (radius/second). **ω** is converted from round per minute (RPM) of electric motor which was given by

$$\boldsymbol{\omega = \frac{RPM \times 60}{2\pi}}$$

Where **π** is 3.14159. RPM are 80 rpm from electric motor's specification. So **ω** is equal to 8.37 rad/s. Then, torque was calculated from above equation which equal to 2.9868 Newton meters. Force (Newton) that electric motor could generate was given by

$$\boldsymbol{F = T/r}$$

Where T was 2.9868 Newton meters and r is a radius of eccentric piece which equal to 0.03 meters. Thus, force that electric motor can generate is 99.56 Newton.

Normally, electric motor had only fifty percent efficiency of calculated data. So, estimate expected force from electric motor is 49.48 Newton.

4.2.2 To calculate length of the lever arm

Eight kilograms load was converted to newton by using the equation below.

$$\sum \vec{F} = mg$$

Where m is a weigh of the subject which is 8 kilograms in this study and g is gravitational constant (9.81 m/s). So, force in this study is 78.48 Newton.

Moment (M) of both sides of the pivot axle is equal which is shown as formula below.

$$\sum M\ (Clockwise) = \sum M\ \ (Anticlockwise)$$

Where M is a moment (NM) which was given by

$$\sum \boldsymbol{M} = \vec{\boldsymbol{F}} \cdot \boldsymbol{d}$$

Where d is a distance from the pivot axle. We combined above formulas and get the formula shown below

$$\boldsymbol{mg} \cdot \boldsymbol{d(s)} = \vec{\boldsymbol{F}}\ \boldsymbol{(motor)} \cdot \boldsymbol{d(l)}$$

Where d_l is a distance of the lever arm from the pivot axle to the eccentric piece that was connected with electric motor, and d_s is a distance of the lever arm from the pivot axle to the load. The formula was rearranged to find the ratio of short and long of the lever arm.

$$\frac{\boldsymbol{d(l)}}{\boldsymbol{d(s)}} = \frac{\boldsymbol{mg}}{\vec{\boldsymbol{F}}\ \boldsymbol{(motor)}}$$

Where mg and F (motor) is 78.48 Newton and 49.48 Newton, respectively from above calculation. So, d_l/ d_s are approximately 5/3. Lever arm was 400 mm and divided into 5/3 ratio. Thus, d_l is 250 mm and d_s is 150 mm.

4.2.3 Specification of this FTM

Round per minute (RPM): RPM was specified by the electric motor which is 80 rpm in this study.

Motor's load efficiency: If this system is assumed to have no error, it could add up to 16 kilograms load.

Load to specimens: The load was specified by 40 percent of the average cadaveric body weight of 8 kilograms in the present study.

Stress's nomenclature: Nomenclature describing test parameters involved in cyclic stress testing are shown in Figure 32. Depending on frequency that was used while testing, the lower frequency the higher stress contact time.

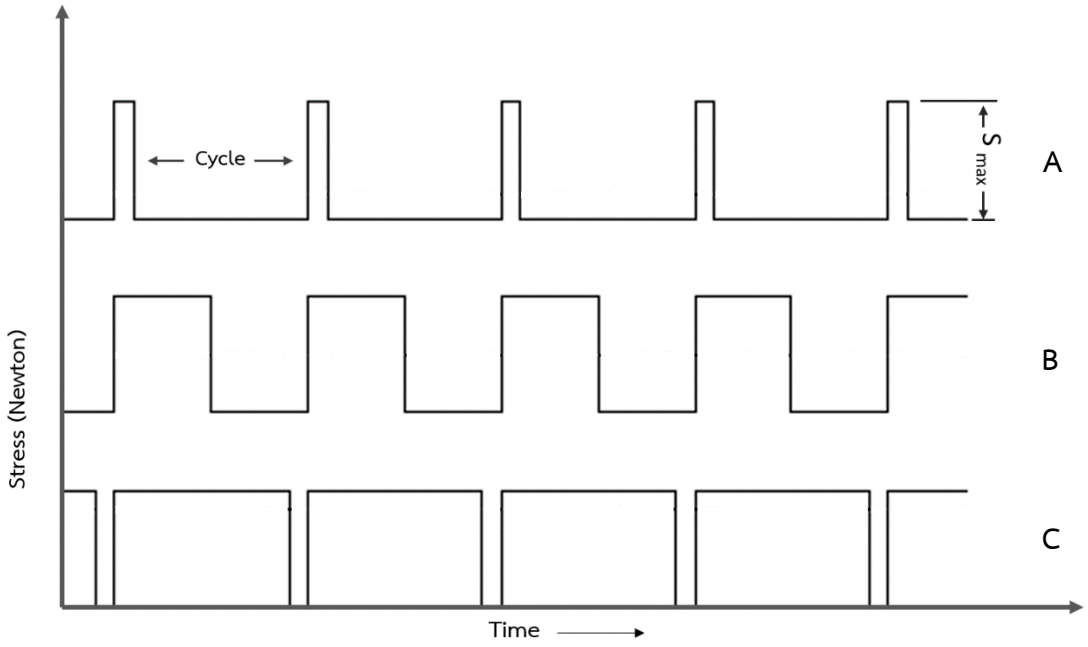

Figure 32 Stress's nomenclature of various testing frequency. (A) Stress's nomenclature of high frequency testing. (B) Stress's nomenclature of medium frequency testing. (C) Stress's nomenclature of low frequency testing.

4.2.4 Fatigue testing machine (FTM) application

According to above specification, FTM was designed for testing the specimen for the repetitive constant force and frequency. In this machine, constant force can be varied from 1 kilograms (only loading unit) to 16 kilograms (maximum weight that electric motor can drive the system). The height of rotating generator part and connector part were adjusted to set level of the lever arm perpendicular to the specimen and to set level of the conical wedge to be close as possible to the specimen. Purpose of this adjusting is to limit the effect of acceleration factor according to Newton's law which shown as equation below.

$$\vec{F} = m(g + \vec{a})$$

Where a is acceleration which primarily depends on the distance between the conical wedge and the specimen.

In addition, constant frequency was specified by the electric motor which is 80 rounds per minute. Constant force, frequency, the FTM generated Stress's nomenclature are shown in Figure 32.

Because we had designed to use aluminum profile (AP) with T-nut (Figure 24A) and tabbed bracket (Figure 24B) as a scaffolding of the rotating generator part (Figure 12) and the connector part (Figure 12). Consequently, we can adjust the height of both the rotating generator and the connector parts of this machine to be compatible with each specimen. Similarly, the fixator part using both T-nut and tabbed bracket, can also be adjusted. The fixator was designed to be adjustable for variation of the length of the cadaveric vertebral column.

4.3 Fatigue testing analysis

4.3.1 Cycles to failure (Fatigue life)

The data of cycles to failure from fatigue testing (CTF) of cancellous screw with manually applied PMMA group (MP), cancellous screws with syringe application PMMA group (CanP), cortical screws with syringe application PMMA group (CorP), and cortical screws with SOP plate group (SOP) were analyzed by using Shapiro-Wilk test which presented the normal distribution (P=0.201). In addition, the present study used Brown-Forsythe for testing the equality of variance, which found equal variance. Individual data of each specimen from each testing group were shown with mean ± SD of CTF in Table 2.

ANOVA showed significant differences among groups of implants (F=457.006, P=0.0001). Then, Holm-Sidak post hoc was used for multiple comparison test of fatigue life (cycles to failure from fatigue testing), of the manually applied PMMA group (MP), the cancellous screws with PMMA group (CanP), the cortical screws with PMMA group (CorP) and the cortical screws with SOP plate group (SOP).

In the MP group, cycles to failure (6,314 ± 1,727) was significantly less than the CanP group (13,580 ± 1,608; p=0.038), the CorP group (49,550 ± 6,392; p<0.001), and the SOP group (112,820 ± 7,562; p<0.001).

In the CanP group, cycles to failure (13,580 ± 1,608) was significantly less than the CorP group (49,550 ± 6,392; p<0.001), and the SOP group (112,820 ± 7,562; p<0.001).

In the CorP group, cycles to failure (49,550 ± 6,392) was significantly less than the SOP group (112,820 ± 7,562; p<0.001).

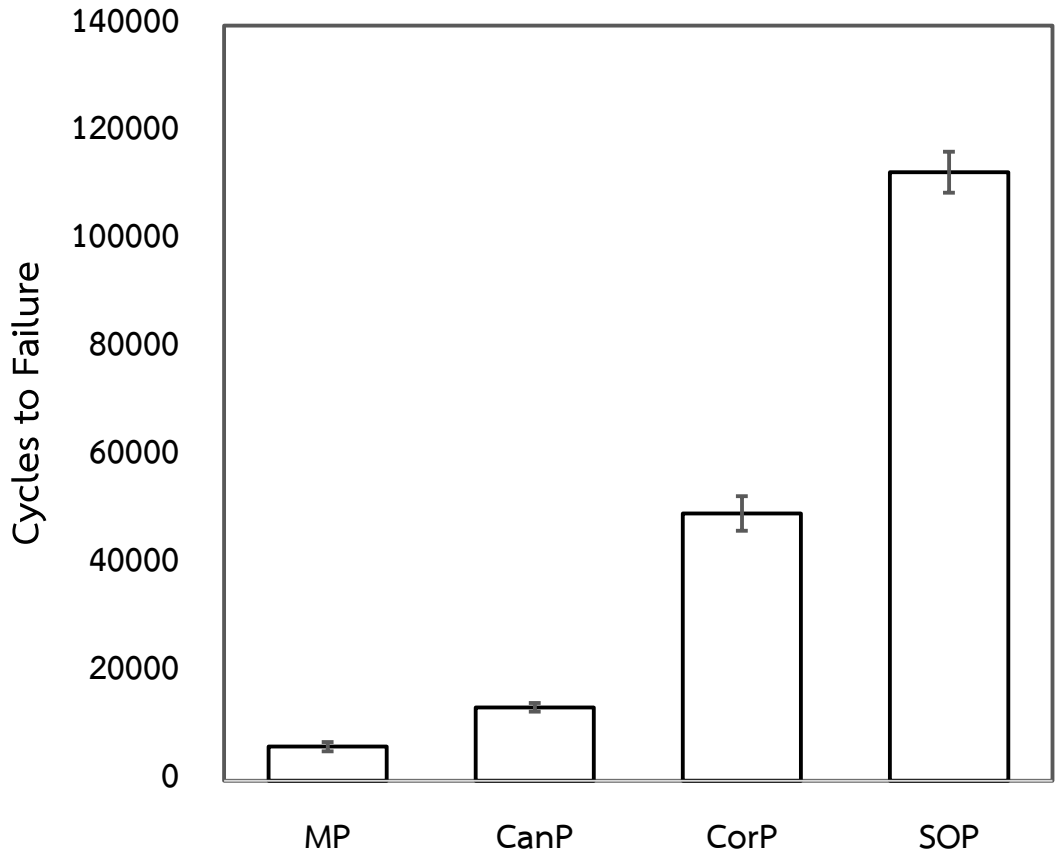

Figure 33 Mean ± SD of cycles to failure withstood by each implant group.

Table 2 Individual data and mean ± SD of cycles to failure (cycles) of each implant group

Cadaver	MP group	CanP group	CorP group	SOP group
1	5,958	14,020	52,145	114,777
2	8,649	12,792	55,195	114,184
3	4,907	12,869	48,485	104,488
4	4,579	12,054	38,964	106,927
5	7,479	16,167	52,963	123,724
Mean ± SD	6,314 ± 1,727[a]	13,580 ± 1,608[b]	49,550 ± 6,392[c]	112,820 ± 7,562[d]

[a,b,c,d] Values within the same row with different superscript are statistically different ($P \leq 0.05$).

4.3.2 Failure mode

4.3.2.1 MP group

In this group, all construction failure occurred through “middle of PMMA bridges” of both sides of the construction. In term of screw, all screws did not show deformation or fissure of the screw (Figure 34) and all screw holes were not dilated.

4.3.2.2 CanP group

The construction failure occurred through “screw neck” of both sides of the construction (Figure 35). In addition, screws which were unbroken, did not present any fissure or deformation. However, all screw holes were markedly dilated (Figure 36).

4.3.2.3 CorP group

Failure of the construction occurred through “PMMA bridges” at the position of screw neck of both sides of the construction (Figure 37). Although all screws were unbroken and did not exhibit any fissure or deformation, the area of PMMA bridge which were unbroken had a crack formation fissure around the screw neck (Figure 38). All screw holes were clearly dilated (Figure 39).

4.3.2.4 SOP group

In this group, construction failure occurred through “screw neck” of both sides of the construction (Figure 40). All screws were unbroken but had a crack formation fissure around the screw neck close to the plate (Figure 41). All screw holes were not dilated.

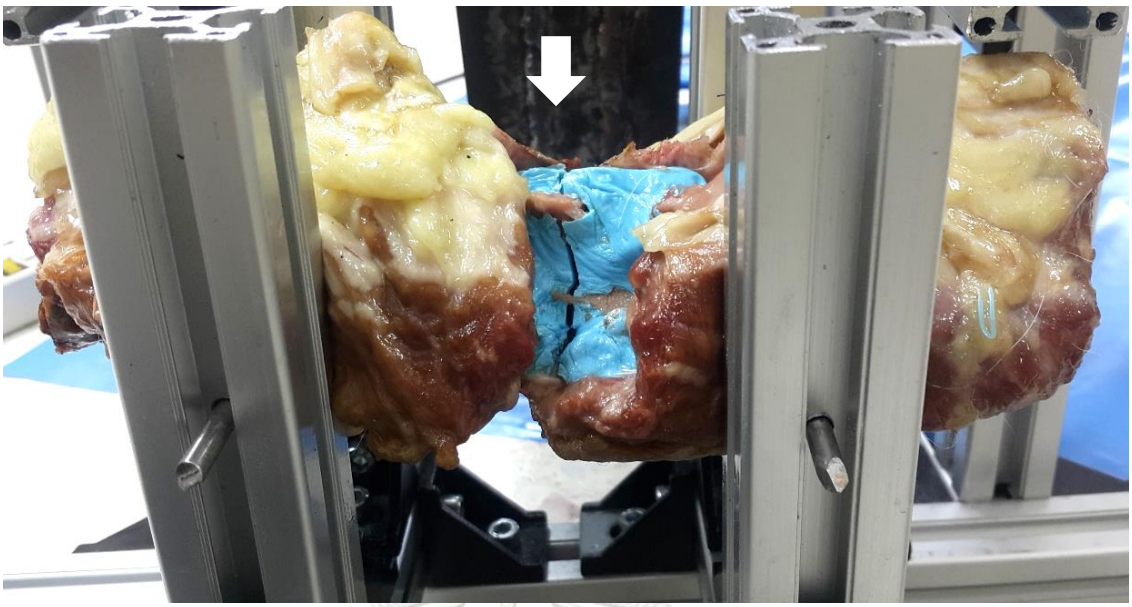

Figure 34 Cracking formation and propagation (white arrow) along PMMA bridge in MP group.

Figure 35 In the CanP group, construction failure occurred through the screw neck of both sides of the construction.

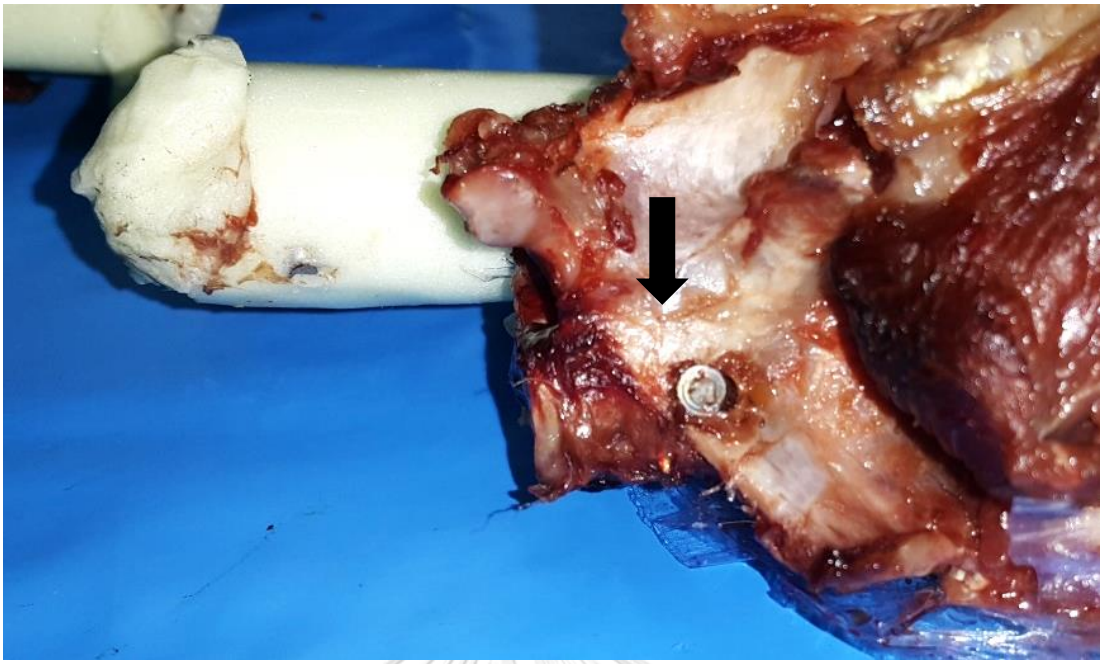

Figure 36 In the CanP group, screw hole was markedly dilated (arrow) after fatigue testing.

Figure 37 In the CorP group, construction failure occurred through PMMA bridges at the position of the screw neck of both sides of the construction.

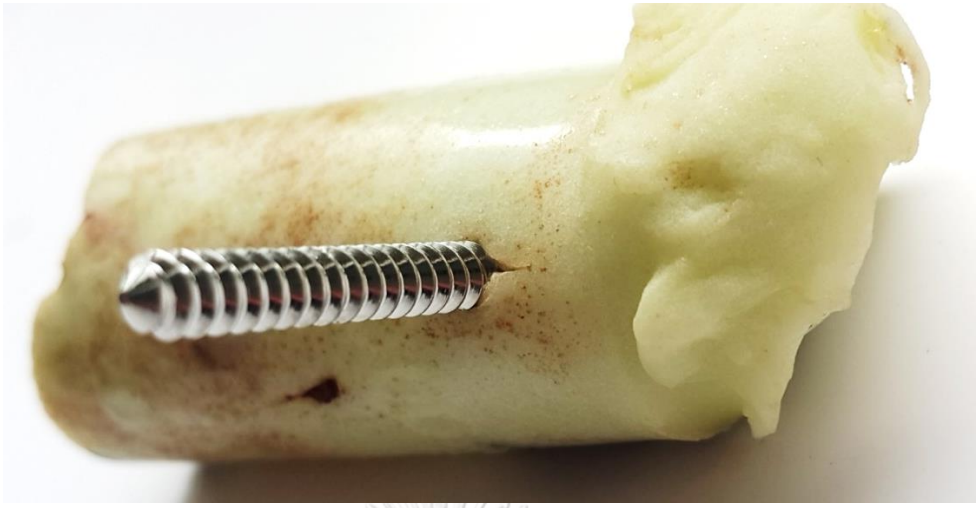

Figure 38 In the CorP group, cracking formation and propagation along PMMA bridge around the screw neck after testing fatigue failure.

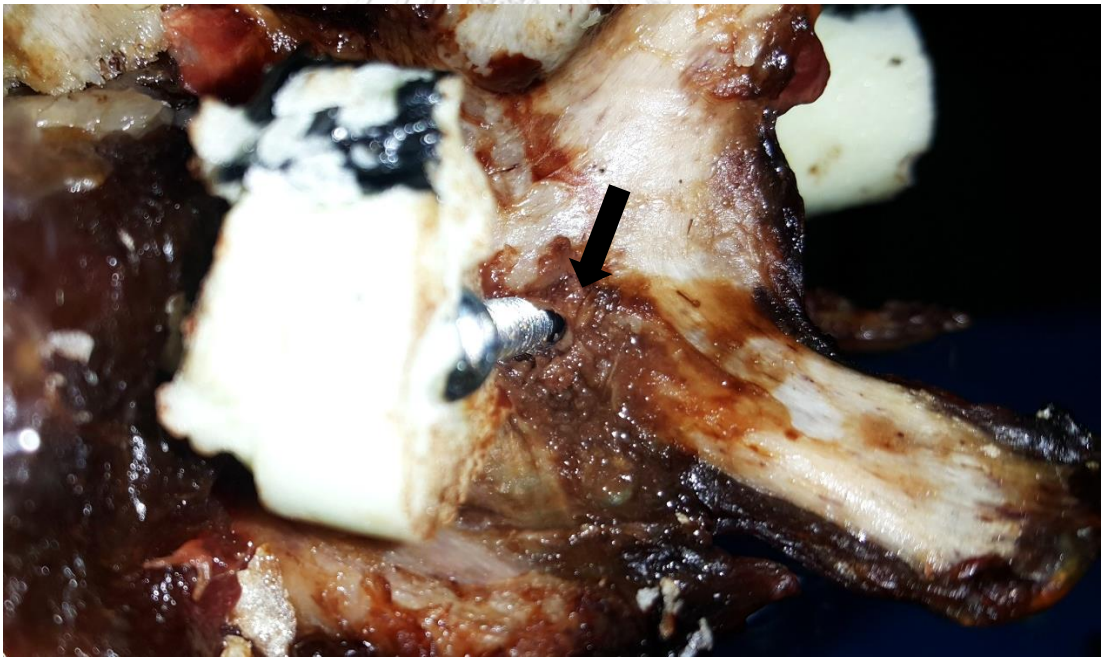

Figure 39 In the CorP group, dilated screw hole (arrow) after testing fatigue failure

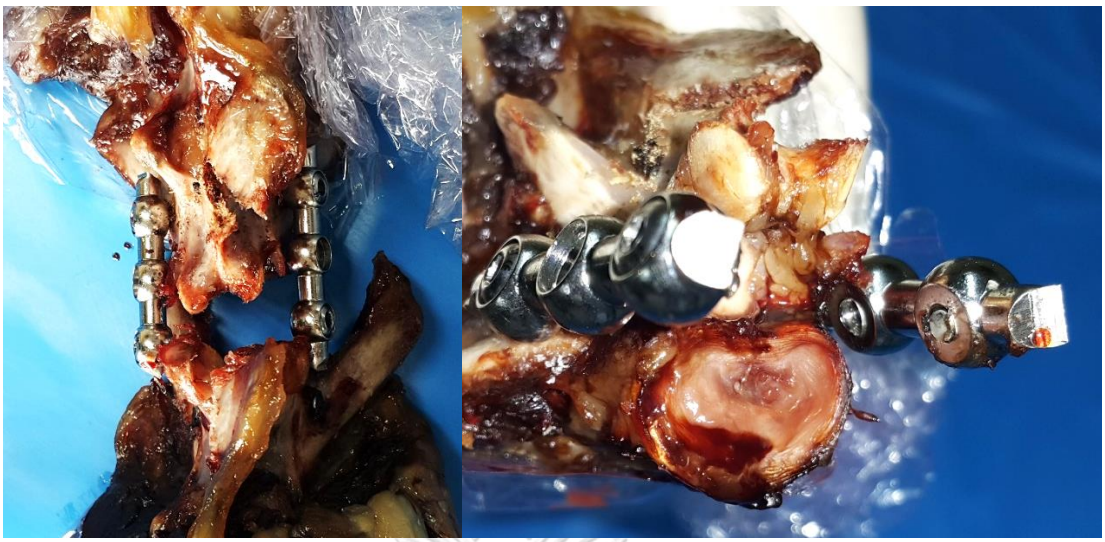

Figure 40 In the SOP group, construction failure occurred through the screw neck of both sides of the construction.

Figure 41 In the SOP group, crack formation fissure around the screw neck (white arrow) and broken screws.

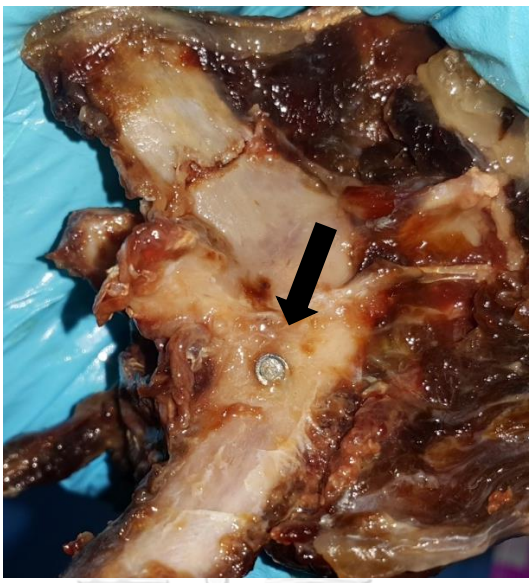

Figure 42 Screw hole of SOP group which was not dilated (arrow) after fatigue testing.

4.4 Correlation study

Specimen's individual data including cycles to failure and cadaveric body weight in each testing group were brought into account to find the correlation.

There was no correlation between cycles to failure (Y) and cadaveric body weight (X) in every testing group. MP group had correlation coefficient = 0.019, R^2 = 0.0004, p = 0.976 and Y = 10.938X + 6086.8 (Figure 43); CanP group had correlation coefficient = 0.310, R^2 = 0.0963, p = 0.611 and Y = 203.66X + 9710.8 (Figure 44); CorP group had correlation coefficient = 0.528, R^2 = 0.2791, p = 0.36 and Y = 919.06X + 30250 (Figure 45); SOP group had correlation coefficient = 0.072, R^2 = 0.0053, p = 0.907 and Y = 115971 - 148.62X (Figure 46).

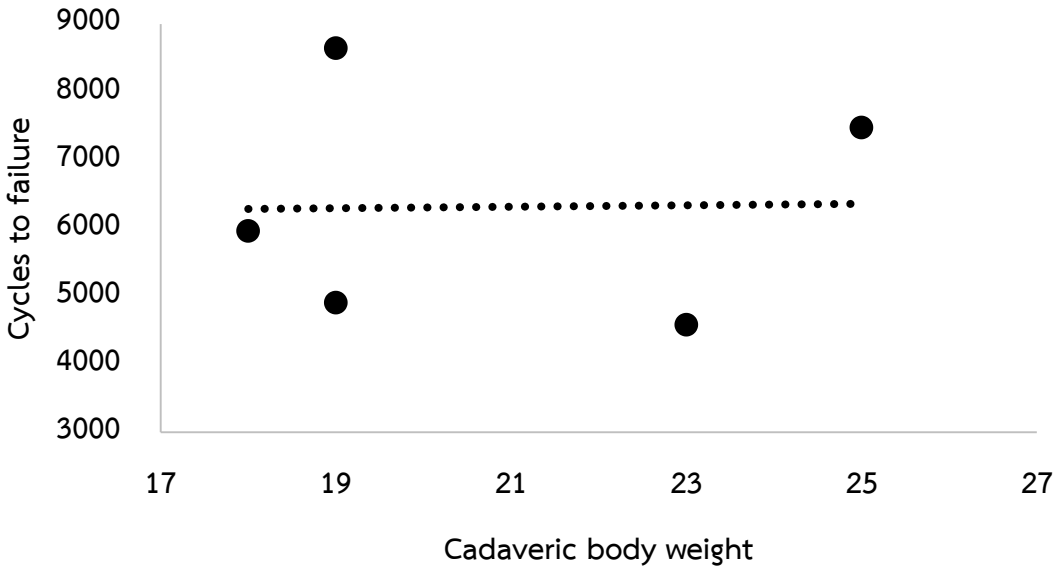

Figure 43 Regression and correlation between cycles to failure (Y) and cadaveric body weight (X) in the cancellous screws with manually applied PMMA group. Correlation was not significant.

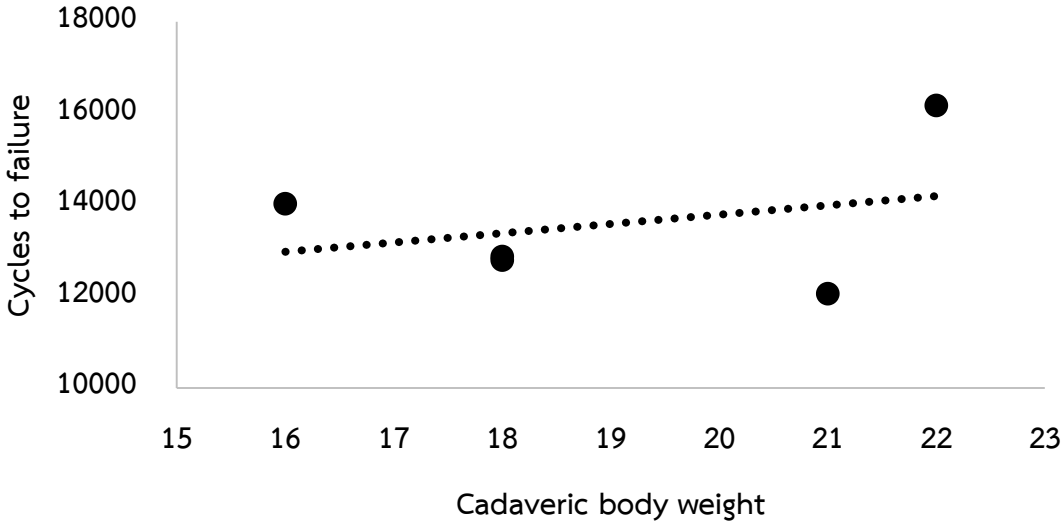

Figure 44 Regression and correlation between cycles to failure (Y) and cadaveric body weight (X) in the cancellous screws with syringe application PMMA group. Correlation was not significant.

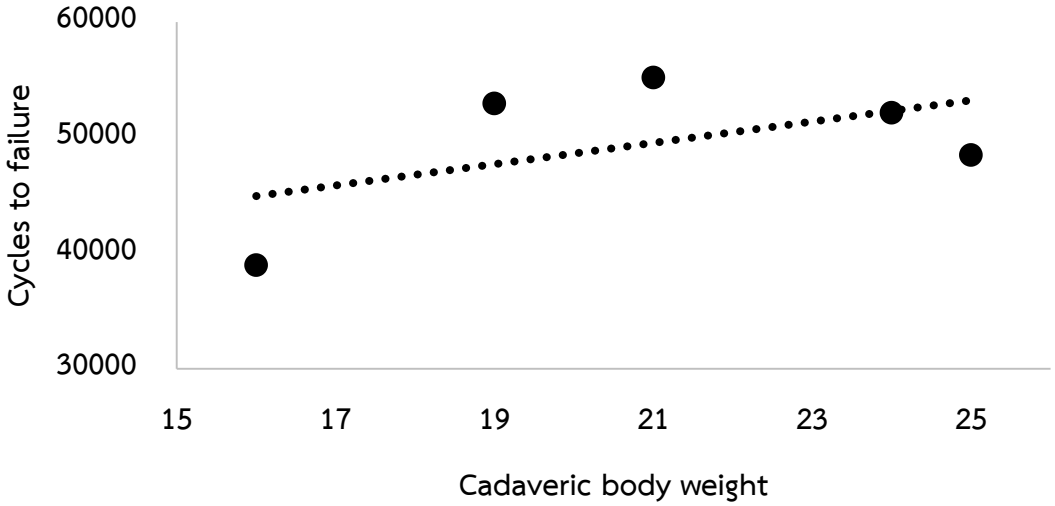

Figure 45 Regression and correlation between cycles to failure (Y) and cadaveric body weight (X) in the cortical screws with syringe application PMMA group. Correlation was not significant.

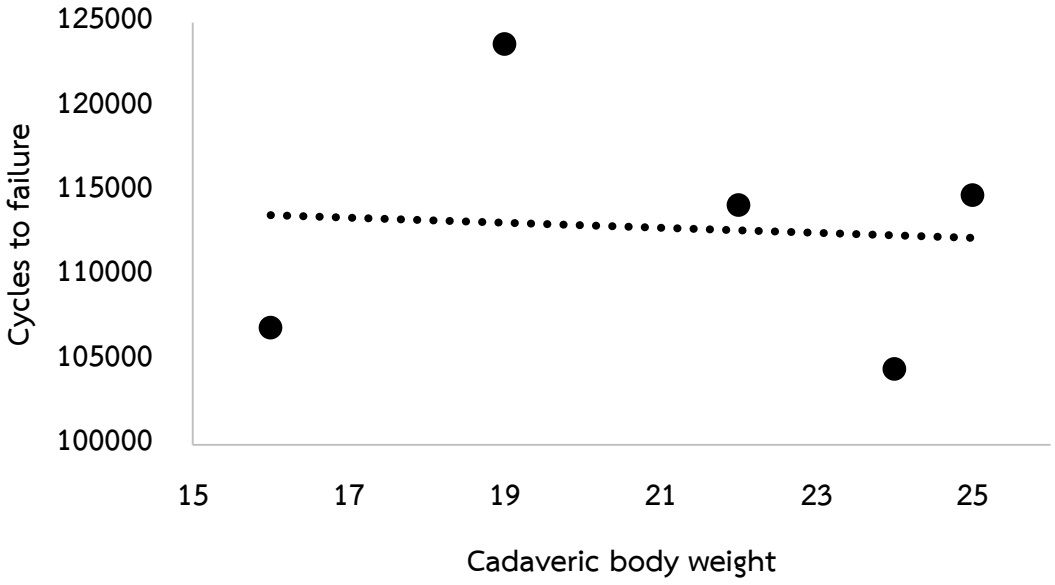

Figure 46 Regression and correlation between cycles to failure (Y) and cadaveric body weight (X) in the cortical screws with SOP plate group. Correlation was not significant.

CHAPTER V

DISCUSSION and CONCLUSION

Our study was performed to evaluate fatigue properties including cycles to failure (CTF) and failure mode (FM) of three PMMA construction and SOP implant. Nowadays, PMMA is a gold standard for treatment the VFL case in dogs and cats (Blass and Iii, 1984; Bruecker and Seim, 1992; Aikawa et al., 2007; Jeffery, 2010). However, SOP plate was also used in VFL treatment but it was unpopular because of its difficult application compared to PMMA construction. Our present study, the fatigue testing machine (FTM) was specially designed in order to test the repetitive cycle loading. Eight kilograms load was used in all testing specimens. The load was calculated from 40 percent of the average body weight of cadavers. Fatigue testing was investigated on cycles to failure and failure mode of each specimen. Moreover, correlation study between cadaveric body weight and CTF was taken into account. The specific design fatigue testing machine cannot change delicate load on the specimen because of the limitation of using iron rod as a load. So, the load was fixed at eight kilograms for every specimen. Other fatigue studies varied the load which mostly calculated from individual cadaveric body weight (Tremolada et al., 2017). However, according to our correlation test which showed that there was no correlation between cadaveric body weight and cycles to failure in the same testing group, we can imply that fixing or varying the load for fatigue testing did not affect the result.

From fatigue study, cycles to failure and failure mode, were investigated in four groups which were MP group, CanP group, CorP group, and SOP group. The specimens were equally divided into each group based on the body weight in order to minimize the effect of the different vertebral column size which might affect the result.

In our study, cycles to failure and failure mode of each testing groups were investigated. Disarticulation and fixation were performed by one person. After fixation, the specimens were kept in -20° C with normal saline soaked sponge (Balligand, 2016). Disarticulating process totally separated L3 and L4 vertebrae in order to obviously detect mode of failure when construction failure occurred.

Twenty cadavers were enrolled to our study. There were no statistical differences of cadaveric body weight and age among testing groups.

Cycles to failure of the MP group (6,314 ± 1,727 cycles) was significantly less than the CanP group (13,580 ± 1,608 cycles; p=0.038), the CorP group (49,550 ± 6,392 cycles; p<0.001), and SOP group (112,820 ± 7,562 cycles; p<0.001). For the failure mode study, the failure occurred at the middle of PMMA bridge in the MP group. Consequently, we hypothesized that using PMMA via manually applied may increase porosity inside the PMMA bridge. In term of using PMMA as manually applied, it must not be applied at the doughing stage because at this stage it has high viscosity. Jasty et al. (1990) reported that the high viscosity stage of PMMA was difficult to remove the air inside the bridge. Therefore, the increasing of porosity inside the PMMA caused significantly reduction of cycles to failure (Linden, 1989). Furthermore, if duration of application is too long, especially with high viscosity PMMA, laminations or folds would occur in the cement mantle, which could reduce fatigue life (cycles to failure) of PMMA (Oh et al., 1983).

Cycles to failure of the CanP group (13,580 ± 1,608 cycles) was significantly less than the CorP group (49,550 ± 6,392 cycles; p<0.001) and the SOP group (112,820 ± 7,562 cycles; p<0.001). Failure mode of this group appeared at the screw neck. Rouleau et al. (1994) reported that there was numerous factors influencing the fatigue properties of an orthopedic implant, including material composition, implant processing history (i.e., cold working, annealing, and forging), implant machining, surface finishing and implant geometry (most particularly, the core diameter of the screw). Mazzocca (1998) described that the core diameter of the screw was the main factor of its strength in bending because the cross-sectional moment of inertia was proportional to the cube of the implant radius. Small increasing in core diameter can lead bending and fatigue strengths to be increased in exponential character. Another study also demonstrated that smaller core diameter screw had fatigue life significantly shorter than larger core diameter screw of the same material (Merk et al., 2001). Moreover, the outer diameter and thread design of the screw subsidized only tiny to its stiffness and strength (SM Perren, 1992). The present study used the cancellous stainless-steel screw with core diameter of 1.9 mm, which smaller than cortical stainless-steel screw

that had 2.4 mm of core diameter. In this study, the difference of core diameter of the cancellous and cortical screw was 0.5 mm, which was 20 percent of difference; consequently, cortical screws with PMMA group had more cycles to failure than the cancellous screws with PMMA group approximately 400 percent of difference. Thus, the ratio of the CTF difference to the core diameter of screw difference was twenty to one of proportion, which could be indicated that the changing only one percent difference of the core diameter screw can increase twenty-time effect to the cycles to failure.

Cycles to failure of CorP group (49,550 ± 6,392 cycles) was significantly less than only the SOP group (112,820 ± 7,562 cycles; $p<0.001$). Failure mode of this group occurred at the PMMA bridge at the position of screw neck. According to Saha and Pal (1984) and British stainless-steel association, the fatigue limit of PMMA and stainless-steel were 8.8 MPa and 270 MPa, respectively. Therefore, in the fatigue strength point of view, PMMA was thirty times weaker than stainless-steel. Thus, comparing between the CorP group and the SOP group, the SOP group had fatigue life more than the CorP group. The SOP group had a pure stainless-steel construction, while the CorP group had a construction that was mixed of PMMA and stainless-steel. According to the result that PMMA bridge was broken at the screw neck position, it could indicate that PMMA was the weakest point of the construction. From the result of the CanP group, failure mode occurred at the cancellous stainless-steel screw neck which could be explained that when core diameter of the screw was large enough, the weakest point might be at the PMMA instead of the cancellous screw.

Cycles to failure of the SOP group was 112,820 ± 7,562 cycles. Failure mode occurred at the cortical stainless-steel screw neck. It could indicate that in the 3.5 mm SOP construction, which was a maximum size of SOP system, the cortical stainless-steel screw was the weakest point of this construction. But breaking of 3.5 mm screw neck in the SOP construction means that SOP plate could tolerate cycles to failure more than that used in this study. So, if the screw diameter of this construction was increased, it might increase cycles to failure.

According to the results in the present study, one theory that could be apprehensible is theory of “Stress Concentration”. A stress concentration (regularly termed stress raisers or stress risers) is a site in a construction where stress is concentrated. The more stress concentration increased the less fatigue life or cycles to failure has occurred due to correlation between stress concentration factor and fatigue life. Any constructions that is reduced in area or has geometric discontinuities (notched or heterogeneity) will have a localized increase in stress which will finally cause the construction failure via a propagating crack. So, homogeneity (unnotched) of construction makes the construction stronger and has more fatigue life due to the force could be evenly distributed over it (Pilkey, 2008). All constructions that were used in the present study could be divided to two compartments which were bridging and bone anchoring compartments. Both compartments could be defined size of notch (heterogeneity level) which was shown in table 3. There are two factors that need to be concerned when the construction failure occurs. They were fatigue properties and homogeneity of the material used in the construction. About fatigue properties of material, the more fatigue limit the more fatigue life (cycles to failure). Thus, in ‘pure’ stainless-steel material construction as the SOP group, the fatigue life was depended on size and position of the notch which cause stress concentration in that area. The weakest point of SOP group was a small notched cortical screw which had more stress concentration than the SOP plate. However, in mixed material construction groups including MP, CanP and CorP groups; we found that even though stainless-steel had more fatigue limit than PMMA, but sometimes it was broken as shown in the CanP group. In the CanP group, the weakest point of the construction was a cancellous screw because the homogeneity effect overcame the fatigue property effect. Homogeneity of PMMA was increased by using syringe application technique. Cancellous screw had a big notch which was a deep root thread. So, in the CorP group, the construction had more homogeneity (smaller notch) than the CanP construction because cortical screw had root thread shallower than cancellous screw. The shallow root thread decreases the stress concentration effect at the screw thread according to the equation below;

$$\sigma\,(\max) = \sigma\left(1 + 2\sqrt{\frac{a}{\rho}}\right)$$

Where ρ is the radius of curvature of the crack tip, a is a half of length of the thread depth of screw and σ (max) is a stress concentration (Newton). The ratio of the σ (max) to σ of the gross cross-section is a stress concentration factor. In the CorP construction, the homogeneity effect did not overcome the fatigue property effect, so, the weakest point of this construction was a PMMA bridge because PMMA had less fatigue limit than stainless-steel. In the construction which the homogeneity effect did not overcome the fatigue property effect, the failure position was an area that connected to two materials together which was at the screw neck position on the PMMA bridge in CorP construction. Moreover, PMMA bridge in MP construction had the big notch due to using manually applied of PMMA as mentioned previously. Thus, MP construction was broken at the middle of PMMA bridge because of low fatigue limit and low homogeneity effect of PMMA from manually applied.

Table 3 Homogeneity of bridging and bone anchoring compartment of all stabilization construction in this study

	Stabilization Construction	
	Bridging compartment	**Bone anchoring compartment**
MP	Big notched PMMA*	Big notched cancellous screw
CanP	Small notched PMMA	Big notched cancellous screw*
CorP	Small notched PMMA*	Small notched cortical screw
SOP	Small notched SOP plate	Small notched cortical screw*

*Compartment that cause construction failure

In conclusion, manually applied PMMA with 3.5 mm cancellous screw, which is currently the surgical standard of care for VFL cases, was not recommended to use. According to the result of MP group, this technique abates the homogeneity and increase in stress concentration in the middle of PMMA bridge. So, PMMA bridge was the weakest point of this construction and caused this construction to have low cycles to failure. However, even though changing application technique to the syringe technique, the construction still had less cycles to failure as well because stress concentration occurred at the cancellous screw thread instead. Even though CorP construction had more cycles to failure but the cortical screw did not provide the resistance property of the screw pull out effect which is one of the most important causes of implant failure in VFL cases. Changing application technique by using syringe and increasing size of cancellous screw might be the solution of this weakness. But the vertebral body size need to be concerned as a limitation of increasing the screw size. Based on the result of this study, SOP plate might be a standard of care for VFL in dogs which had the most cycles to failure.

Advantages of the study

The study of cycles to failure and failure mode of four testing groups provides useful information and new knowledges of fatigue properties of all testing constructions. Although, the specific design fatigue testing machine is not a standard machine for testing fatigue properties of implants, but some confidentially understandable information in using PMMA, cancellous stainless-steel screw, cortical stainless-steel screw and SOP plate system in vertebral fracture and luxation model is obtained from this machine.

Limitation of the study

This fatigue testing machine tested fatigue failure only on dorsoventral manner. Although, dorsoventral bending is the major force that affects the implant after stabilization, but it also has axial compression, tension, rotation, shearing and lateral bending force. This specific fatigue testing was not a standard method for testing fatigue life which could generate S/N curve to find the fatigue or endurance limit. Nevertheless, trend of result was similar to that from standard fatigue testing machine in the cycles to failure or fatigue life point of view.

Conclusion

SOP group has the most cycles to failure which is greater than CorP group, CanP group and MP group in declining order. The weakest point of each construction group was a manually applied PMMA, 3.5 mm cancellous screw neck, syringe technique application PMMA and 3.5 mm cortical screw in MP, CanP, CorP and SOP group, respectively which defined from failure mode.

Suggestion

Besides the construction tested in our present study, there are more constructions that were used in VFL cases such as locking compression plate and pedicle screw system. The pedicle screw system is a standard of care for human VFL cases. Pedicle screw is a pure titanium construction which has a lot of fatigue limit. So, further study should be done on the fatigue testing by using pedicle screw system as one of the testing group.

REFERENCES

Aikawa T, Kanazono S, Yoshigae Y, Sharp NJ and Munana KR 2007. Vertebral stabilization using positively threaded profile pins and polymethylmethacrylate, with or without laminectomy, for spinal canal stenosis and vertebral instability caused by congenital thoracic vertebral anomalies. Vet Surg. 36(5): 432-441.

Ajaxon I and Persson C 2014. Compressive fatigue properties of a commercially available acrylic bone cement for vertebroplasty. Biomech Model Mechanobiol. 13(6): 1199-1207.

Arbi M 1998. Stabilization Techniques: Thoracolumbar Spine. In: AO ASIF Principles in Spine Surgery. ed. J Webb (ed). Berlin: Springer. 83-122.

Arora M, Chan EK, Gupta S and Diwan AD 2013. Polymethylmethacrylate bone cements and additives: A review of the literature. World J Orthop. 4(2): 67-74.

Bagley RS 2000. Spinal fracture or luxation. The Veterinary clinics of North America. Small animal practice. 30(1): 133-153, vi-vii.

Balligand M 2016. Setting up ex-vivo biomechanics studies. 18th ESVOT Congress 2016, London:40.

Blass CE and Iii HBS 1984. Spinal Fixation in Dogs Using Steinmann Pins and Methylmethacrylate. Veterinary Surgery. 13(4): 203-210.

Boyer H 1986. Fatigue testing. In: Atlas of Fatigue Curves. ed. H Boyer (ed). Ohio: ASM International. 1-26.

Brinckmann P, Biggemann M and Hilweg D 1988. Fatigue fracture of human lumbar vertebrae. Clinical Biomechanics. 3: i-S23.

Bruce CW, Brisson BA and Gyselinck K 2008. Spinal fracture and luxation in dogs and cats: a retrospective evaluation of 95 cases. Vet Comp Orthop Traumatol. 21(3): 280-284.

Bruecker KA 1996. Principles of vertebral fracture management. Seminars in veterinary medicine and surgery (small animal). 11(4): 259-272.

Bruecker KA and Seim HB, 3rd 1992. Principles of spinal fracture management. Seminars in veterinary medicine and surgery (small animal). 7(1): 71-84.

Carberry CA, Flanders JA and Dietz AE 1989. Nonsurgical management of thoracic and lumbar spinal fractures and fracture/luxations in the dog and cat: a review of 17 cases. . J Am Anim Hosp Assoc. 25: 43–45.

Cronier P, Pietu G, Dujardin C, Bigorre N, Ducellier F and Gerard R 2010. The concept of locking plates. Orthopaedics & Traumatology: Surgery & Research. 96(4): S17-S36.

Eveleigh R 2001. Principles of bone cement mixing. British journal of perioperative nursing : the journal of the National Association of Theatre Nurses. 11(1): 18-20.

Farahmand B 1997. Conventional Fatigue (High- and Low-Cycle Fatigue). In: Fatigue and Fracture Mechanics of High Risk Parts. ed. J Glassco (ed). New York: Chapman & Hall. 13-102.

Feeney DA and Oliver JE 1980. Blunt spinal trauma in the dog and cat: neurologic, radiologic, and therapeutic correlations. Journal of the American Animal Hospital Association. 16(5): 664-668.

Fluehmann G, Doherr MG and Jaggy A 2006. Canine neurological diseases in a referral hospital population between 1989 and 2000 in Switzerland. J Small Anim Pract. 47(10): 582-587.

Garcia JN, Milthorpe BK, Russell D and Johnson KA 1994. Biomechanical study of canine spinal fracture fixation using pins or bone screws with polymethylmethacrylate. Vet Surg. 23(5): 322-329.

Gordon-Evans W 2015. Vertebral fracture repair. In: Complications in Small Animal Surgery. ed. D Griffon (ed). New Jersey: Wiley-Blackwell. 611.

Graham J, Pruitt L, Ries M and Gundiah N 2000. Fracture and fatigue properties of acrylic bone cement: the effects of mixing method, sterilization treatment, and molecular weight. J Arthroplasty. 15(8): 1028-1035.

Hall DA, Snelling SR, Ackland DC, Wu W and Morton JM 2015. Bending strength and stiffness of canine cadaver spines after fixation of a lumbar spinal fracture-

luxation using a novel unilateral stabilization technique compared to traditional dorsal stabilization. Vet Surg. 44(1): 94-102.

Heisel C, Norman T, Rupp R, Pritsch M, Ewerbeck V and Breusch SJ 2003. In vitro performance of intramedullary cement restrictors in total hip arthroplasty. Journal of biomechanics. 36(6): 835-843.

Jasty M, Davies JP, O'Connor DO, Burke DW, Harrigan TP and Harris WH 1990. Porosity of various preparations of acrylic bone cements. Clinical orthopaedics and related research. (259): 122-129.

Jeffery ND 2010. Vertebral Fracture and Luxation in Small Animals. The Veterinary clinics of North America. Small animal practice. 40(5): 809-828.

Khaled SM, Charpentier PA and Rizkalla AS 2011. Physical and mechanical properties of PMMA bone cement reinforced with nano-sized titania fibers. J Biomater Appl. 25(6): 515-537.

Krauss MW, Theyse LF, Tryfonidou MA, Hazewinkel HA and Meij BP 2012. Treatment of spinal fractures using Lubra plates. A retrospective clinical and radiological evaluation of 15 cases. Vet Comp Orthop Traumatol. 25(4): 326-331.

Linden U 1989. Fatigue properties of bone cement. Comparison of mixing techniques. Acta orthopaedica Scandinavica. 60(4): 431-433.

Lumb WV and Brasmer TH 1970. Improved spinal plates and hypothermia as adjuncts to spinal surgery. Journal of the American Veterinary Medical Association. 157(3): 338-342.

Marioni-Henry K, Vite CH, Newton AL and Van Winkle TJ 2004. Prevalence of diseases of the spinal cord of cats. Journal of veterinary internal medicine. 18(6): 851-858.

Mazzocca A 1998. Principles of internal fixation. In: Skeletal Trauma. ed. B Browner (ed). Philadelphia: WB Saunders. 287–348.

Merk BR, Stern SH, Cordes S and Lautenschlager EP 2001. A fatigue life analysis of small fragment screws. Journal of orthopaedic trauma. 15(7): 494-499.

Mjoberg B, Rydholm A, Selvik G and Onnerfalt R 1987. Low- versus high-viscosity bone cement. Fixation of hip prostheses analyzed by roentgen stereophotogrammetry. Acta orthopaedica Scandinavica. 58(2): 106-108.

Ness MG 2009. The effect of bending and twisting on the stiffness and strength of the 3.5 SOP implant. Veterinary and Comparative Orthopaedics and Traumatology (VCOT). 22(2): 132-136.

Nickel R 1986. The locomotor system of the domestic mammals. In: Verlag P. Parey.

Oh I, Bourne RB and Harris WH 1983. The femoral cement compactor. An improvement in cementing technique in total hip replacement. The Journal of bone and joint surgery. American volume. 65(9): 1335-1338.

Olby N 2010. The Pathogenesis and Treatment of Acute Spinal Cord Injuries in Dogs. Veterinary Clinics of North America: Small Animal Practice. 40(5): 791-807.

Olby N 2015. Spinal trauma. In: Small Animal Neurological Emergencies. ed. S Platt (ed). Northwestern: CRC press. 383-397.

Pilkey WD 2008. Definition and design relations. In: Peterson's Stress Concentration Factors. 3 ed. DF Pilkey (ed). Manhattan: John Wiley & Sons.

Rouleau JP, Blasier RB, Tsai E and Goldstein SA 1994. Cannulated hip screws: a study of fixation integrity, cut-out resistance, and high-cycle bending fatigue performance. Journal of orthopaedic trauma. 8(4): 293-299.

Rouse GP and Miller JI 1975. The use of methylmethacrylate for spinal stabilization. Journal of the American Animal Hospital Association. 11(4): 418-425.

Saha S and Pal S 1984. Mechanical properties of bone cement: A review. Journal of Biomedical Materials Research. 18(4): 435-462.

Shores A 1992. Spinal trauma. Pathophysiology and management of traumatic spinal injuries. The Veterinary clinics of North America. Small animal practice. 22(4): 859-888.

Shores A, Nichols C, Rochat M, Fox SM, Burt GJ and Fox WR 1989. Combined Kirschner-Ehmer device and dorsal spinal plate fixation technique for caudal lumbar vertebral fractures in dogs. Journal of the American Veterinary Medical Association. 195(3): 335-339.

SM Perren JC, Baumgar F 1992. Technical and biomechanical aspects of screws used for bone surgery. Int J Orthop Trauma. 2(2): 31-48.

Smit TH 2002. The use of a quadruped as an in vivo model for the study of the spine - Biomechanical considerations. European Spine Journal. 11(2): 137-144.

Sturges BK, Kapatkin AS, Garcia TC, Anwer C, Fukuda S, Hitchens PL, Wisner T, Hayashi K and Stover SM 2016. Biomechanical Comparison of Locking Compression Plate versus Positive Profile Pins and Polymethylmethacrylate for Stabilization of the Canine Lumbar Vertebrae. Vet Surg. 45(3): 309-318.

Tremolada G, Lewis DD, Paragnani KL, Conrad BP, Kim SE and Pozzi A 2017. Biomechanical comparison of a 3.5-mm conical coupling plating system and a 3.5-mm locking compression plate applied as plate-rod constructs to an experimentally created fracture gap in femurs of canine cadavers. American journal of veterinary research. 78(6): 712-717.

Vaishya R, Chauhan M and Vaish A 2013. Bone cement. Journal of Clinical Orthopaedics and Trauma. 4(4): 157-163.

Voss K and Montavon PM 2004. Tension band stabilization of fractures and luxations of the thoracolumbar vertebrae in dogs and cats: 38 cases (1993-2002). Journal of the American Veterinary Medical Association. 225(1): 78-83.

Weh 2011. Spinal fractures and luxations. In: Veterinary Surgery Small Animal. ed. K Tobias (ed). London: Saunders. 487-503.

Wheeler JL, Lewis DD, Cross AR and Sereda CW 2007. Closed Fluoroscopic-Assisted Spinal Arch External Skeletal Fixation for the Stabilization of Vertebral Column Injuries in Five Dogs. Veterinary Surgery. 36(5): 442-448.

Zand MS, Goldstein SA and Matthews LS 1983. Fatigue failure of cortical bone screws. Journal of biomechanics. 16(5): 305-311.

Zotti A, Gianesella M, Gasparinetti N, Zanetti E and Cozzi B 2011. A preliminary investigation of the relationship between the "moment of resistance" of the canine spine, and the frequency of traumatic vertebral lesions at different spinal levels. Res Vet Sci. 90(2): 179-184.

APPENDIX

VITA

Mister Mingrath Mekavichai was born on January 30th, 1991 in Muscat, Oman. He achieved his bachelor degree of Doctor of Veterinary Medicine (D.V.M.) from the Faculty of Veterinary Science, Chulalongkorn University in 2015. After graduation, he enrolled in the Master's Degree program of the Department of Veterinary Surgery, Chulalongkorn University. His special interest is on Veterinary Neurology.